

Article

Genome-Wide Characterization of DGATs and Their Expression Diversity Analysis in Response to Abiotic Stresses in *Brassica napus*

Xiangzhen Yin ^{1,2,†}, Xupeng Guo ^{1,2,†}, Lizong Hu ^{1,2,3}, Shuangshuang Li ^{1,2}, Yuhong Chen ¹, Jingqiao Wang ⁴, Richard R.-C. Wang ⁵, Chengming Fan ^{1,*} and Zanmin Hu ^{1,2,*}

¹ State Key Laboratory of Plant Cell and Chromosome Engineering, Institute of Genetics and Developmental Biology, Innovation Academy for Seed Design, Chinese Academy of Sciences, Beijing 100101, China; yinxiangzhen1985@163.com (X.Y.); guoxvpeng@163.com (X.G.); hulizong@126.com (L.H.); ss.li@genetics.ac.cn (S.L.); yhchen@genetics.ac.cn (Y.C.)

² College of Advanced Agriculture Sciences, University of Chinese Academy of Sciences, Beijing 100049, China

³ College of Biology and Agriculture, Zhoukou Normal University, Zhoukou 466001, China

⁴ Institute of Economical Crops, Yunnan Agricultural Academy, Kunming 650205, China; jingqiao_wang@126.com

⁵ United States Department of Agriculture, Agricultural Research Service, Forage and Range Research Laboratory, Utah State University, Logan, UT 84322-6300, USA; richard.wang@usda.gov

* Correspondence: cmfan@genetics.ac.cn (C.F.); zmhu@genetics.ac.cn (Z.H.); Tel./Fax: +86-010-64807626 (Z.H.)

† These authors contributed equally to this work.



Citation: Yin, X.; Guo, X.; Hu, L.; Li, S.; Chen, Y.; Wang, J.; Wang, R.R.-C.; Fan, C.; Hu, Z. Genome-Wide Characterization of DGATs and Their Expression Diversity Analysis in Response to Abiotic Stresses in *Brassica napus*. *Plants* **2022**, *11*, 1156. <https://doi.org/10.3390/plants11091156>

Academic Editor: María Ferriol Molina

Received: 1 April 2022

Accepted: 22 April 2022

Published: 25 April 2022

Publisher's Note: MDPI stays neutral with regard to jurisdictional claims in published maps and institutional affiliations.



Copyright: © 2022 by the authors. Licensee MDPI, Basel, Switzerland. This article is an open access article distributed under the terms and conditions of the Creative Commons Attribution (CC BY) license (<https://creativecommons.org/licenses/by/4.0/>).

Abstract: Triacylglycerol (TAG) is the most important storage lipid for oil plant seeds. Diacylglycerol acyltransferases (DGATs) are a key group of rate-limiting enzymes in the pathway of TAG biosynthesis. In plants, there are three types of DGATs, namely, DGAT1, DGAT2 and DGAT3. *Brassica napus*, an allotetraploid plant, is one of the most important oil plants in the world. Previous studies of *Brassica napus* DGATs (BnaDGATs) have mainly focused on BnaDGAT1s. In this study, four DGAT1s, four DGAT2s and two DGAT3s were identified and cloned from *B. napus* ZS11. The analyses of sequence identity, chromosomal location and collinearity, phylogenetic tree, exon/intron gene structures, conserved domains and motifs, and transmembrane domain (TMD) revealed that BnaDGAT1, BnaDGAT2 and BnaDGAT3 were derived from three different ancestors and shared little similarity in gene and protein structures. Overexpressing *BnaDGATs* showed that only four BnaDGAT1s can restore TAG synthesis in yeast H1246 and promote the accumulation of fatty acids in yeast H1246 and INVSc1, suggesting that the three *BnaDGAT* subfamilies had greater differentiation in function. Transcriptional analysis showed that the expression levels of *BnaDGAT1s*, *BnaDGAT2s* and *BnaDGAT3s* were different during plant development and under different stresses. In addition, analysis of fatty acid contents in roots, stems and leaves under abiotic stresses revealed that P starvation can promote the accumulation of fatty acids, but no obvious relationship was shown between the accumulation of fatty acids with the expression of *BnaDGATs* under P starvation. This study provides an extensive evaluation of BnaDGATs and a useful foundation for dissecting the functions of BnaDGATs in biochemical and physiological processes.

Keywords: *Brassica napus*; DGAT; expression pattern; abiotic stresses; fatty acids

1. Introduction

Triacylglycerol (TAG), the major component of vegetable oils, consists of three fatty acids esterified to a glycerol backbone. In plants, TAG is not only mainly stored in seeds, functioning as an energy reservoir to facilitate germination and early seedling growth, but also provides precursors for membrane biosynthesis and lipid signaling, which are crucial for normal plant growth and development [1–3]. DGAT (diacylglycerol acyltransferase, EC2.3.1.20), the key rate-limiting enzyme of the Kennedy pathway for TAG biosynthesis,

catalyzes the final and committed step in this pathway by transferring an acyl group from acyl-CoA to the *sn*-3 position of *sn*-1,2-diacylglycerol (DAG) [4–6]. In plants, DGATs are classified into three distinct types, namely, DGAT1, DGAT2 and DGAT3, which were first identified in *Arabidopsis* [7], castor (*Ricinus communis*) [8] and tung tree (*Vernicia fordii*) [9] and peanut (*Arachis hypogaea*) [10], respectively. Since then, many varieties of the three DGAT types have been characterized in different species, such as olive [11,12], tobacco [13], soybean [14–16], peanut [17,18], canola [19–21], tung tree [9], sunflower [22], *Tropaeolum majus* [23], maize [24] and cotton [25].

As the final enzyme in TAG biosynthesis, DGAT1s are critical to oilseed development [7,19,26] and have been highlighted as a genetic engineering target to increase storage lipid production in plants [13,27–30]. In addition, DGAT1s have been demonstrated to be associated with normal growth [30–33] and abiotic stress responses [34–42]. Plant DGAT1s and DGAT2s, although catalyzing the same enzyme activity, have distinct physiological functions [9,43]. Plant DGAT2s were characterized from species that produce oils enriched with unusual FAs, such as *R. communis* [8], *V. fordii* [9,43] and ironweed (*Vernonia galamensis*) [44], which produce TAGs enriched in ricinoleic acid, α -eleostearic acid and vernolic acid, respectively. *B. napus* DGAT2s (*Bna*DGAT2s) were shown to play an important role in the accumulation of erucic acid in *Brassica napus* in one study [45]. Some plant DGAT3s were also confirmed to be involved in TAG synthesis. For example, *Ah*DGAT3-1 was demonstrated to be specific for 1,2-diacylglycerol rather than hexadecanol, glycerol-3-phosphate, monoacylglycerol, lysophosphatidic acid and lysophosphatidylcholine and to prefer oleoyl-CoA as an acyl donor compared to palmitoyl- and stearoyl-CoAs [10]. Heterologous expression of *Ah*DGAT3-3 could restore TAG biosynthesis with preferential incorporation of unsaturated C18 fatty acids into lipids in yeast H1246 [17]. Similar to *Arabidopsis*, recombinant purified *At*DGAT3 produced from *Escherichia coli*, although very unstable, exhibits DGAT activity in vitro [46], and transient expression of *At*DGAT3 in *Nicotiana benthamiana* confirmed its involvement in TAG synthesis and specificity towards 18:3 and 18:2 FAs [47]. Overexpression of *Gh*DGAT3D improved the oil content in *Arabidopsis* seeds [25].

The expression patterns of DGATs are very helpful in analyzing their functions. In plants, most DGAT1s are expressed widely in different tissues (roots, stems, leaves, flowers, developing pods, seedlings, germinated seeds, etc.), especially in developing seeds [7,14,15,20,48,49]. The expression levels of *B. napus* DGAT1s (*Bna*DGAT1s) during the silique development may be different in diverse germplasm sources, and higher numbers and levels of expression of *Bna*DGAT1s are correlated with high oil germplasm [50]. The expression patterns of DGAT2s are diverse in different species. Olive *Oe*DGAT2 is highly expressed in mature and ageing tissues, for example, in the late stages of anther and ovary development [11]. Soybean *Gm*DGAT2D is mainly expressed in flowers [14]. Small individual changes in the relative expression of *Bna*A.DGAT2s were discovered, but the isoforms' expression decreased as a general trend in the late developmental stages for MAPLUS (nonedible, high-erucic acid), whereas it remained on an even level in MONOLIT (edible, low-erucic acid) [45]. Cytosolic DGAT3 was first purified and identified from developing peanut cotyledons and was highly expressed between 8 and 24 DAF (days after flowering) but not detected in leaves, roots or 30-DAF seeds [10].

Stresses have an important effect on plant DGAT expression. The expression levels of DGAT1s were increased under freezing stress conditions [41,42]. The expression of soybean *Gm*DGAT2D could be promoted by cold, heat or ABA treatment but inhibited by jasmonate and insect infestation [14].

B. napus, one of the most important oil plants in the world, is an allotetraploid species (AACC, $2n = 38$) that contains two sets of homologous chromosomes derived from its diploid progenitors, *Brassica rapa* (AA, $2n = 20$) and *Brassica oleracea* (CC, $2n = 18$) [51–53]. It was expected that there may be four copies for a gene in *B. napus*. The copy number, sequence structure, relationship between sequence and function and spatial and temporal expression patterns of *Bna*DGAT1s, *Bna*DGAT2s and *Bna*DGAT3s in *B. napus* have not been systematically analyzed. In addition, various kinds of stresses, such as P starvation, low

N, drought and salinity, have important influences on the growth and development of *B. napus*, and the expression of *BnaDGATs* in response to these stresses has important value for analyzing their functions, which have not been reported.

In this study, four DGAT1s, four DGAT2s and two DGAT3s were identified and annotated widely in the *B. napus* genome. Further characterizations were performed with the analyses of sequence identity, chromosomal location and collinearity, phylogenetic tree, exon/intron gene structures, conserved domains and motifs and transmembrane domain (TMD). The TAG-synthesizing abilities were tested by overexpressing *BnaDGATs* in both yeast H1246 and INVSc1. Transcriptomic analysis and qRT-PCR were performed to detect the expression patterns of *BnaDGATs* in different tissues and under different stresses. The *cis*-elements upstream of the start codons of *BnaDGATs* were investigated by PlantCARE. Moreover, the contents of fatty acids in roots, stems and leaves under the stresses of P starvation, low N, drought and salinity were analyzed by GS-MS. This study provides an extensive evaluation of *BnaDGATs* and provides a useful foundation for dissecting the functions of *BnaDGATs* in lipid metabolism and growth under stress in *B. napus*.

2. Results

2.1. Identification and Annotation of DGAT Family Members in *B. napus*

The CDS and protein sequences of AtDGAT1, AtDGAT2 and AtDGAT3 from the *Arabidopsis* database TAIR (<http://www.arabidopsis.org/> (accessed on 25 March 2020)) were used as queries for the BLAST search in the two *B. napus* databases (GENOSCOPE, <https://www.genoscope.cns.fr/brassicanapus/> (accessed on 25 March 2020) and BnPIR, <http://cbi.hzau.edu.cn/bnapus> (accessed on 2 March 2021)). The results showed that three *BnaDGAT1s*, four *BnaDGAT2s* and two *BnaDGAT3s* in GENOSCOPE and four *BnaDGAT1s*, four *BnaDGAT2s* and two *BnaDGAT3s* in BnPIR were detected (Table 1). To further confirm the *BnaDGAT* family members, the primers (Table S1) for cloning them were designed according to the genomic DNA and CDSs in the two *B. napus* databases, and four *BnaDGAT1s*, four *BnaDGAT2s* and two *BnaDGAT3s* (Table 1) were then cloned and identified from *B. napus* ZS11. Simultaneously, five *DGAT* genes in *Brassica rapa*, five in *Brassica oleracea*, five in *Brassica nigra* and ten in *Brassica juncea* were classified using the same BLAST search in the *Brassica* Database (BRAD, <http://brassicadb.cn/#/> (accessed on 11 October 2021)), as well as eight in *Brassica carinata* in the *Brassica* Genomics Database (BGD, <http://brassicadb.bio2db.com/> (accessed on 11 October 2021)) (Table 1). In addition, *DGAT* genes in other typical plants, *Arachis hypogaea*, *Glycine max*, *Ricinus communis*, *Medicago truncatula*, *Jatropha curcas*, *Oryza sativa*, *Zea mays*, *Setaria italica* and *Brachypodium distachyon*, were also detected by the same BLAST search in their corresponding genome databases (Table S2). All sequences of the CDS, genomic DNA and protein of *DGATs* in *B. napus* and other typical plants in this study are presented in Tables S3–S6.

The amino acid sequences of *BnaDGAT* genes were characterized: the protein length ranged from 317 AA to 510 AA, and the molecular weight (MW) ranged from 35.64 kDa to 57.96 kDa (Table 2). Moreover, the isoelectric point (pI) values ranged from 7.75 to 8.90, which showed that these proteins are alkaline (Table 2). Moreover, the subcellular localization signals of four *BnaDGAT1s* and four *BnaDGAT2s* were detected in the endoplasmic reticulum, as were the *DGAT1s* and *DGAT2s* of the other plants in this study (Table 2 and Table S7). No subcellular localization signals of *DGAT3s* were detected in *B. napus* or other plants (Table 2 and Table S7).

Identity analysis of *BnaDGATs*, *BraDGATs* and *BolDGATs* was performed by the Clustal W method based on nucleotide sequences and amino acid sequences (Table S8). The results showed that the three *DGAT* subfamilies shared very low identity with each other subfamily (8.2% to 17.2%), while the similarities among eight *DGAT1s*, eight *DGAT2s* and four *DGAT3s* were high (72.4% to 100%) at the amino acid sequence level. The similarity between every *BnaDGAT* in the A subgenome and its orthologous one in the C subgenome was higher than 96%. The identity of *DGATs* based on nucleotide sequences was similar to that based on amino acid sequences (Table S8).

Table 1. Members of the DGAT family in *A. thaliana* and six *Brassica* species forming U's triangle according to their genome databases.

<i>Arabidopsis thaliana</i>	<i>Brassica napus</i>		<i>Brassica rapa</i>	<i>Brassica oleracea</i>	<i>Brassica nigra</i>	<i>Brassica juncea</i>	<i>Brassica carinata</i>
	<i>Brassica_napus_v4.1</i>	ZS11	Brara_Chiifu_V3.0	Braol_JJS_V2.0	Brani_Ni100_V2	Braju_tum_V1.5	
AtDGAT1 At2G19450	BnaA07g36000D	BnaA07G0011800ZS	BraA07g001370.3C	—	—	BjuA046403-A07	—
	BnaAnng30990D	BnaA09G0121200ZS	BraA09g011830.3C	—	—	BjuA017169-A09	—
	—	—	—	—	BniB03g068710.2N	BjuB029654-B03	BcaB03g16730
	—	—	—	—	BniB04g025020.2N	BjuB028615-B04	BcaB07g31608
	BnaCnng52810D	BnaC07G0026200ZS	—	BolC07g002350.2J	—	—	BcaC04g22852
	—	BnaC09G0126800ZS	—	BolC09g013760.2J	—	—	BcaC06g36576
AtDGAT2 At3G51520	BnaA01g19390D	BnaA01G0206700ZS	BraA01g022340.3C	—	—	BjuA005097-A01	—
	BnaA03g41350D	BnaA03G0420700ZS	BraA03g045590.3C	—	—	BjuA042315-A03	—
	—	—	—	—	BniB02g074660.2N	BjuB048735-B02	BcaC06g33029
	—	—	—	—	BniB05g021740.2N	BjuB013221-B05	BcaNung00379
	BnaC01g23350D	BnaC01G0259700ZS	—	BolC01g027430.2J	—	—	—
	BnaC07g32270D	BnaC07G0393500ZS	—	BolC07g044710.2J	—	—	—
AtDGAT3 At1G48300	BnaA08g03400D	BnaA08G0039500ZS	BraA08g004520.3C	—	—	BjuA014363-A08	—
	—	—	—	—	BniB07g007860.2N	BjuB045147-B07	BcaB04g17451
	BnaC08g46660D	BnaC08G0049200ZS	—	BolC08g005290.2J	—	—	BcaC07g37153

AtDGATs were extracted from the *Arabidopsis* database (TAIR, <http://www.arabidopsis.org/> (accessed on 25 March 2020)); BnaDGATs in *Brassica_napus_v4.1* were selected from *Brassica napus* Genome Browser (<http://www.genoscope.cns.fr/brassicnapus/> (accessed on 25 March 2020)); ZS11 indicates the gene locus IDs of BnaDGATs in *B. napus* ZS11 genome database (BnPIR; <http://cbi.hzau.edu.cn/bnapus/index.php> (accessed on 2 March 2021)); *B. rapa*, *B. oleracea*, *B. nigra* and *B. juncea* DGATs were blasted in the *Brassica* database (BRAD, <http://brassicadb.cn/#/> (accessed on 11 October 2021)); *B. carinata* DGATs were derived from the *Brassica* Genomics Database (BGD, <http://brassicadb.bio2db.com/> (accessed on 11 October 2021)). The concept of U's triangle described natural allopolyploidization events in *Brassica* using three diploids (*B. rapa* (A genome), *B. nigra* (B), and *B. oleracea* (C) and three derived allotetraploids (*B. juncea* (AB genome), *B. napus* (AC), and *B. carinata* (BC)) [51].

Table 2. Cloning and characterization of the members of *BnaDGAT* family.

Scheme	Gene Name	Gene Locus ID	Chromosome Location	Protein				Putative Promoter
				AA	pI	Mw (Da)	Subcellular Location	
DGAT1	<i>BnaA.DGAT1.a</i>	BnaA07G0011800ZS	A07:935,937-939,473	504	8.75	57,743.80	E.R.	1759 bp
	<i>BnaA.DGAT1.b</i>	BnaA09G0121200ZS	A09:7,271,130-7,274,477	503	8.09	57,241.36	E.R.	1488 bp
	<i>BnaC.DGAT1.a</i>	BnaC07G0026200ZS	C07:4,705,347-4,708,653	501	8.43	57,538.87	E.R.	1657 bp
	<i>BnaC.DGAT1.b</i>	BnaC09G0126800ZS	C09:9,270,137-9,273,644	510	8.20	57,958.08	E.R.	1500 bp
DGAT2	<i>BnaA.DGAT2.a</i>	BnaA01G0206700ZS	A01:12,907,146-12,908,853	368	8.77	41,813.30	E.R.	836 bp
	<i>BnaA.DGAT2.b</i>	BnaA03G0420700ZS	A03:22,826,130-22,827,759	367	8.32	41,280.40	E.R.	775 bp
	<i>BnaC.DGAT2.a</i>	BnaC01G0259700ZS	C01:20,695,151-20,696,870	319	8.88	36,103.24	E.R.	2151 bp
	<i>BnaC.DGAT2.b</i>	BnaC07G0393500ZS	C07:51,188,778-51,190,546	317	7.75	35,636.69	E.R.	1973 bp
DGAT3	<i>BnaA.DGAT3</i>	BnaA08G0039500ZS	A08:3,290,776-3,291,925	356	8.90	38,476.61	None	1660 bp
	<i>BnaA.DGAT3</i>	BnaC08G0049200ZS	C08:4,709,675-4,710,823	356	8.84	38,184.10	None	1459 bp

Gene Name shows the names of BnaDGATs annotated according to the nomenclature principles of *Brassica* genes (genus-species-genome-gene name-locus-allele) [54]. The gene locus IDs, chromosome locations and orientation of *BnaDGATs* were derived from the *B. napus* ZS11 genome database (BnPIR; <http://cbi.hzau.edu.cn/bnapus/index.php> (accessed on 2 March 2021)). The isoelectric point (pI) and molecular weight (Mw) of BnaDGAT proteins were predicted using the ProtParam tool (<https://web.expasy.org/protparam/> (accessed on 22 October 2021)). Subcellular localization patterns of BnaDGAT1s and BnaDGAT2s were predicted, and the results showed that they were located in the endoplasmic reticulum (E.R.), whereas no BnaDGAT3s were evaluated using ProtComp v.9.0 in softberry (<http://linux1.softberry.com/> (accessed on 22 October 2021)).

2.2. Chromosomal Location and Collinearity Analysis

Chromosomal location (Table 2 and Figure S1A) analysis showed four *BnaDGAT1s* distributed on chromosomes A07, A09, C07 and C09; four *BnaDGAT2s* distributed on chromosomes A01, A03, C01 and C07 and that two *BnaDGAT3s* were distributed on chromosomes A08 and C08. In *B. rapa*, five *BraDGATs* were located on *B. rapa* chromosomes A07, A09, A01, A03 and A08 (Figure S1B) and in *B. oleracea*, five *BolDGATs* were located on *B. oleracea* chromosomes C07, C09, C01, C07 and C08 (Figure S1C). Five *BnaDGAT* loci on the *B. napus* A subgenome were highly parallel with five *BraDGAT* loci on the *B. rapa* A genome, and five *BnaDGAT* loci on the *B. napus* C subgenome were highly parallel with five *BolDGAT* loci on the *B. oleracea* C genome, which suggested that *B. napus* inherited and retained all the *DGAT* genes of *B. rapa* and *B. oleracea*.

The results of gene synteny analysis (Figure 1A) showed that four *BnaDGAT1s*, four *BnaDGAT2s* and two *BnaDGAT3s* might be duplicated genes, suggesting that *BnaDGAT* genes were frequently duplicated during oilseed rape evolution. The results of comparative synteny of *DGAT* gene pairs among *A. thaliana*, *B. oleracea*, *B. rapa*, *B. napus* and *B. nigra* (Figure 1B) showed that *AtDGAT1*, *AtDGAT2* and *AtDGAT3* had collinearity relationships with two *BolDGAT1s*/two *BraDGAT1s*/four *BnaDGAT1s*/two *BniDGAT1s*, two *BolDGAT2s*/two *BraDGAT2s*/four *BnaDGAT2s*/two *BniDGAT2s* and one *BolDGAT3*/one *BraDGAT3*/two *BnaDGAT3s*/one *BniDGAT3*, respectively.

Moreover, the synonymous mutations (Ks), nonsynonymous mutations (Ka) and Ka/Ks ratios of the orthologous *DGAT* gene pairs between *B. napus* and *A. thaliana* and the paralogous *BnaDGAT* gene pairs were evaluated (Table 3). The results showed that all of the Ka/Ks ratios of these gene pairs were lower than 1 (Table 3), indicating that these gene pairs experienced strong purifying selective pressure. The duplication time of these gene pairs was presumed using the formula $T = Ks/2R$, with R (1.5×10^{-8}) representing neutral substitution per site per year. The results showed that the duplication times of the orthologous *DGAT* gene pairs between *B. napus* and *A. thaliana* ranged from 10.67 MYA to 20.11 MYA (Table 3), with an average value of 15.06 MYA. These results indicated that *DGATs* of *B. napus* diverged from *A. thaliana* ~16 MYA, which was consistent with the recent whole-genome triplication event that occurred approximately 9–15 MYA or even 28 MYA [55]. The corresponding duplication times of the paralogous *BnaDGAT* gene pairs ranged from 1.37 to 12.78 MYA, with an average value of 8.36 MYA (Table 3). Two peaks of duplication times were observed in *B. napus*: one peak (1.37–3.57 MYA) represented the duplication time of these genes, which occurred during the divergence of the A genome and C genome of *Brassica*, and the other peak (10.95–12.78 MYA), representing a duplication time of ~10 MYA, corresponded to the *Brassica* whole-genome triplication event (9–15 MYA) [55]. Therefore, the processes of *B. napus* speciation and *Brassica* whole-genome triplication likely played important roles in the divergence of the *BnaDGAT* duplicated genes in *B. napus*.

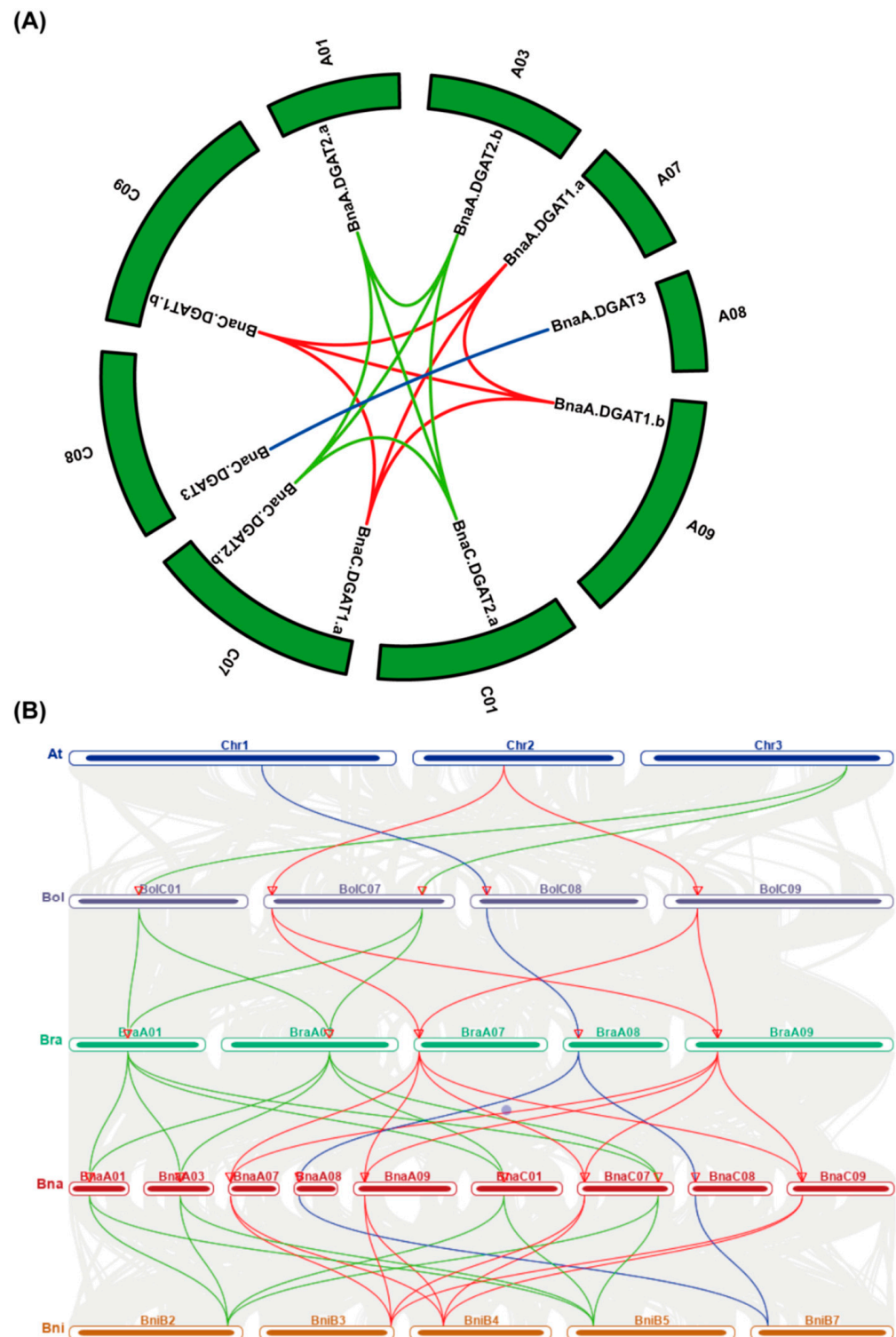


Figure 1. Synteny analysis of DGATs in *Arabidopsis thaliana*, *Brassica oleracea*, *Brassica rapa*, *Brassica napus* and *Brassica nigra*. **(A)** Synteny analysis of the *BnaDGAT* family in *B. napus*. Red-, green- and blue-colored lines indicate the *BnaDGAT1* subfamily, *BnaDGAT2* subfamily and *BnaDGAT3* subfamily genes, respectively; **(B)** Synteny analysis of DGATs between *A. thaliana*, *B. oleracea*, *B. rapa*, *B. napus* and *B. nigra*. Red, green and blue lines indicate the syntenic *DGAT1*, *DGAT2* and *DGAT3* gene pairs between the denoted species, respectively. In the background, the grey line represents collinear blocks.

Table 3. Ks/Ka values between *BnaDGAT* and their paralogous gene pairs in *Brassica napus* and their orthologous gene pairs in *Arabidopsis*.

	Gene_1	Gene_2	Ka	Ks	Ka/Ks	Duplication Time (MYA)	Average (MYA)
Orthologous gene pairs	<i>AtDGAT1</i>	<i>BnaA.DGAT1.a</i>	0.062	0.320	0.194	10.67	15.06
	<i>AtDGAT1</i>	<i>BnaA.DGAT1.b</i>	0.064	0.400	0.161	13.33	
	<i>AtDGAT1</i>	<i>BnaC.DGAT1.a</i>	0.064	0.347	0.184	11.56	
	<i>AtDGAT1</i>	<i>BnaC.DGAT1.b</i>	0.060	0.415	0.145	13.82	
	<i>AtDGAT2</i>	<i>BnaA.DGAT2.a</i>	0.098	0.486	0.201	16.21	
	<i>AtDGAT2</i>	<i>BnaA.DGAT2.b</i>	0.123	0.448	0.275	14.92	
	<i>AtDGAT2</i>	<i>BnaC.DGAT2.a</i>	0.099	0.495	0.200	16.51	
	<i>AtDGAT2</i>	<i>BnaC.DGAT2.b</i>	0.124	0.436	0.284	14.55	
	<i>AtDGAT3</i>	<i>BnaA.DGAT3</i>	0.081	0.568	0.143	18.92	
	<i>AtDGAT3</i>	<i>BnaC.DGAT3</i>	0.086	0.603	0.142	20.11	
Paralogous gene pairs	<i>BnaA.DGAT1.a</i>	<i>BnaA.DGAT1.b</i>	0.056	0.346	0.161	11.52	8.36
	<i>BnaA.DGAT1.a</i>	<i>BnaC.DGAT1.a</i>	0.003	0.041	0.064	1.37	
	<i>BnaA.DGAT1.a</i>	<i>BnaC.DGAT1.b</i>	0.054	0.329	0.163	10.97	
	<i>BnaA.DGAT1.b</i>	<i>BnaC.DGAT1.a</i>	0.058	0.358	0.162	11.92	
	<i>BnaA.DGAT1.b</i>	<i>BnaC.DGAT1.b</i>	0.007	0.097	0.073	3.22	
	<i>BnaC.DGAT1.a</i>	<i>BnaC.DGAT1.b</i>	0.056	0.328	0.170	10.95	
	<i>BnaA.DGAT2.a</i>	<i>BnaA.DGAT2.b</i>	0.111	0.347	0.321	11.58	
	<i>BnaA.DGAT2.a</i>	<i>BnaC.DGAT2.a</i>	0.009	0.085	0.107	2.83	
	<i>BnaA.DGAT2.a</i>	<i>BnaC.DGAT2.b</i>	0.112	0.372	0.301	12.41	
	<i>BnaA.DGAT2.b</i>	<i>BnaC.DGAT2.a</i>	0.111	0.376	0.296	12.52	
	<i>BnaA.DGAT2.b</i>	<i>BnaC.DGAT2.b</i>	0.010	0.092	0.107	3.07	
	<i>BnaC.DGAT2.a</i>	<i>BnaC.DGAT2.b</i>	0.111	0.383	0.290	12.78	
	<i>BnaA.DGAT3</i>	<i>BnaC.DGAT3</i>	0.019	0.107	0.179	3.57	

2.3. Evolutionary Relationship and Exon/Intron Gene Structure Analysis of *BnaDGATs*

The phylogenetic tree (Figure 2A) showed that three well-supported clades were grouped as the DGAT1 subfamily, DGAT2 subfamily and DGAT3 subfamily. Within the DGAT1 subfamily and DGAT2 subfamily, four *BnaDGAT1s* and four *BnaDGAT2s*, respectively, were grouped more closely with the corresponding DGAT subfamilies of the other five *Brassica* U's triangle species (*B. rapa*, *B. oleracea*, *B. nigra*, *B. juncea* and *B. carinata*) and *Arabidopsis* than to those of the other dicot or monocot plants. Within the DGAT3 subfamily, two *BnaDGAT3s* were grouped more closely to those of *B. oleracea*, *B. rapa*, *B. nigra*, *B. carinata* and *Arabidopsis* than to the corresponding subfamilies of the other dicot or monocot plants. The DGAT1s, DGAT2s and DGAT3s of the four monocot plants were always grouped together, rather than with those of the twelve dicot plants. These results indicated that the duplication events of *DGAT* genes occurred after the divergence of dicot and monocot plants.

The results of the exon/intron gene structures (Figures 2B and S2B and Table S7) revealed that the gene structures of most *DGAT1s*, *DGAT2s* and *DGAT3s* were highly and independently conserved during evolution but confirmed distinct differences among the three *DGAT* subfamilies, suggesting that the three *DGAT* subfamilies evolved separately from three different ancient genes. All four *BnaDGAT1s* have 16 exons as well as *DGAT1s* from most other plants, except *BjuB029654* (13 exons), *BjuB028615* (14 exons) and

BraA07g001370.3C (14 exons). Most *DGAT2s* are generally composed of seven to ten exons. In addition, *BnaA01G0206700ZS* had seven exons and *BnaA03G0420700ZS* had six exons in the *B. napus* database BnPIR (Table S7), but we cloned these genes and confirmed that they (*BnaA.DGAT2.a* and *BnaA.DGAT2.b*) had nine and eight exons, respectively. Members of *DGAT3s* from *B. napus* and the selected plants in this paper contain two exons, except *BcaC07g37153* (four exons), *BjuA014363* (six exons) and *BjuB045147* (five exons).

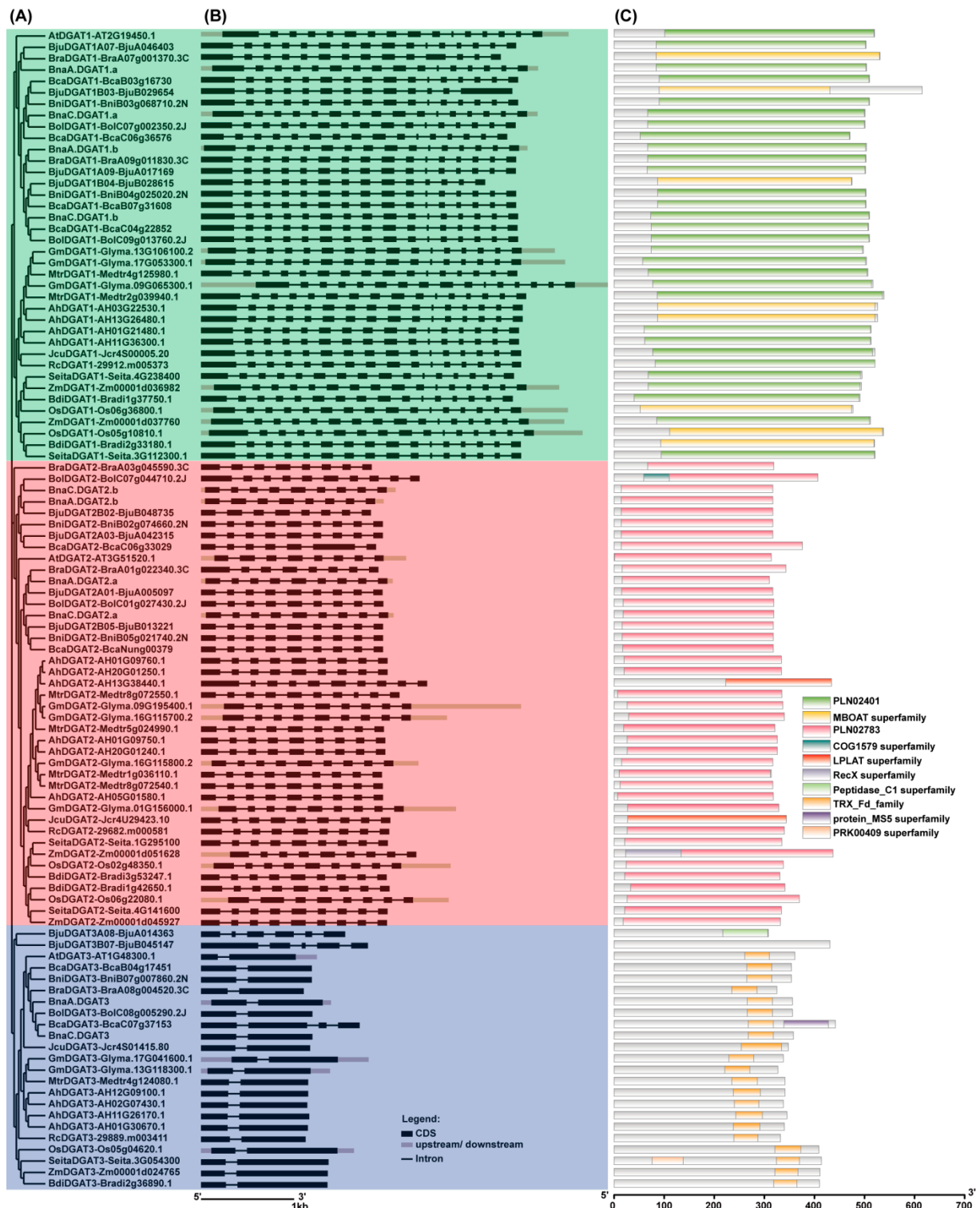


Figure 2. Analyses of phylogenetic tree, gene structures and conserved domains of DGAT family members in *Brassica napus* and other plant species. (A) Phylogenetic tree. DGAT protein sequences

were used to construct the phylogenetic tree by MEGA11 software with the neighbor-joining method and 2000 bootstrap replications; (B) Gene structures. The genomic DNA and CDSs of DGATs were used to construct the gene structures by the Gene Structure Display Serve (GSDS2.0; <http://gsds.gao-lab.org/> (accessed on 20 October 2021)) [56]. Black boxes denote exons within coding regions, and the lines connecting exons represent introns. Grey boxes indicate the upstream or downstream regions of the CDS of DGAT genes. The length of the boxes represents the size of the corresponding exons; (C) Conserved domains. A functional search of the conserved domains was performed using the Conserved Domain Database (CDD) with Batch CD-Search in NCBI. *BnaDGAT1s*, *BnaDGAT2s* and *BnaDGAT3s* were cloned from *B. napus* ZS11. The protein, genomic DNA and CDSs of DGAT family members in *B. oleracea*, *B. rapa*, *B. nigra*, *B. juncea*, *B. carinata*, *A. thaliana*, *A. hypogaea*, *G. max*, *R. communis*, *O. sativa*, *Z. mays*, *S. italica*, *M. truncatula*, *B. distachyon* and *J. curcas* were blasted and selected from their corresponding genome databases (Table S2). All DGAT1s contained the PLN02401 domain (diacylglycerol o-acyltransferase) or the MBOAT domain (membrane-bound O-acyltransferase family). All DGAT2 homologues shared the PLN02783 domain (diacylglycerol o-acyltransferase), except AH13G38440.1 and Jcr4U29423.10, which had an LPLAT superfamily domain. All DGAT3 homologues shared the TRX_Fd_family domain, except BjuB045147 and BjuA014363.

2.4. The Conserved Domains and Motif Analyses

To investigate the conserved motifs and domains, the DGAT proteins from *B. napus* and the other selected plants were predicted by both the Conserved Domain Database (CDD) with Batch CD-Search in NCBI [57] and the MEME program (<https://meme-suite.org/meme/tools/meme> (accessed on 21 October 2021)) (Bailey et al., 2009), as shown in Figures 2C and S3. All DGAT1s contained the PLN02401 domain (diacylglycerol o-acyltransferase) or MBOAT domain (membrane-bound O-acyltransferase family). All DGAT2 homologues shared the PLN02783 domain (diacylglycerol o-acyltransferase), except AH13G38440.1 and Jcr4U29423.10, which had an LPLAT superfamily domain. All DGAT3 homologues shared the TRX_Fd_family domain, except BjuB045147 and BjuA014363.

Additionally, the top 20 conserved motifs were identified in the DGAT proteins (Figure S3). All the DGAT1 homologues shared one motif 2, one motif 3, one motif 7, one motif 8, one motif 9, one motif 12 and one motif 15. All DGAT1 homologues had one motif 1, except BjuB029654 and BjuB028615. All DGAT1 homologues had one motif 4, except BjuB029654 and 29912.m005373. All DGAT1 homologues had one motif 20, except BjuB029654 and Zm00001d036982. All DGAT1 homologues, except BjuA046403, had one motif 13. All DGAT1 homologues of six *Brassica* species, *A. thaliana*, and *A. hypogaea* shared one motif 19. All DGAT2 homologues had one motif 5, one motif 6, one motif 10, one motif 11, one motif 12 and one motif 14. All DGAT2 homologues had one motif 17, except BraA03g045590.3C, AH13G38440.1 and AH05G01580.1. All DGAT2 homologues had one motif 16, except BraA03g045590.3C and AH13G38440.1. All DGAT3 homologues had one motif 18 at their C-terminus, except BjuB045147 and BjuA014363. All DGAT3 homologues shared one or two motifs 15 at their C-terminus, except Os05g04620.1, Seita.3G054300.1 and Zm00001d024765. These results supported the hypothesis that the DGAT1, DGAT2 and DGAT3 subfamilies evolved separately during eukaryote evolution, as demonstrated by the phylogenetic tree and gene structure (Figure 2).

2.5. Putative Transmembrane Domains of DGAT Proteins

The putative transmembrane domains (TMDs) of DGAT proteins from *B. napus* and other plants were predicted by TMHMM (<https://services.healthtech.dtu.dk/service.php?TMHMM-2.0> (accessed on 10 April 2021)) (Figure 3 and Table S7) [58]. Each of the DGAT1s was predicted to harbor seven to ten putative TMDs. For *B. napus*, BnaA.DGAT1.a and BnaC.DGAT1.a had eight putative TMDs, and BnaA.DGAT1.b and BnaC.DGAT1.b shared nine putative TMDs. For most DGAT2s, one to four putative TMDs were detected. Each of four BnaDGAT2s had two putative TMDs at the N-terminus with a large cytosolic

C-terminal domain. There were no putative TMDs in any of the examined DGAT3s, consistent with their soluble nature.

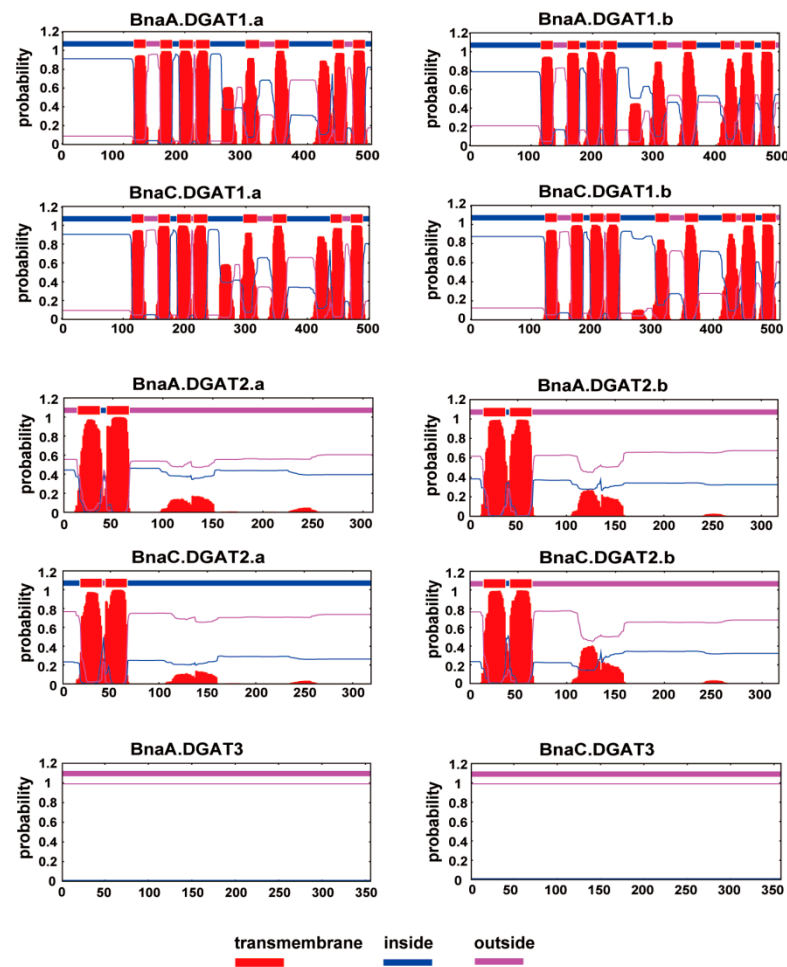


Figure 3. Predicted transmembrane domains (TMDs) of BnaDGATs. Each BnaDGAT1s had eight or nine putative TMDs, and each BnaDGAT2s showed two putative TMDs. However, neither BnaDGAT3 had putative TMDs. The putative TMDs of BnaDGATs were predicted using TMHMM Server v. 2.0 (<https://services.healthtech.dtu.dk/service.php?TMHMM-2.0> (accessed on 10 April 2021)). Regions of BnaDGATs predicted to be located inside or outside the membrane are shown in bold blue and pink lines, respectively.

2.6. Oil Droplets in *S. cerevisiae* H1246 Overexpressing BnaDGATs

DGAT is the rate-limiting enzyme in the last step of TAG synthesis, and TAG is the main component of oil bodies. Therefore, the yeast mutant H1246 (*MAT α are1- Δ ::HIS3, are2- Δ ::LEU2, dga1- Δ ::KanMX4, lro1- Δ ::TRP1 ADE2*) [59] that are defective in TAG biosynthesis were used to determine whether the ten BnaDGATs are able to complement the mutated enzymes and allow the synthesis and accumulation of TAG. As shown in Figure 4, many obvious oil bodies were detected in yeast H1246 overexpressing *BnaDGAT1s*, while no obvious oil bodies were detected in H1246 overexpressing *BnaDGAT2s* and *BnaDGAT3s*, suggesting that only the four BnaDGAT1s were able to re-establish TAG synthesis in yeast H1246.

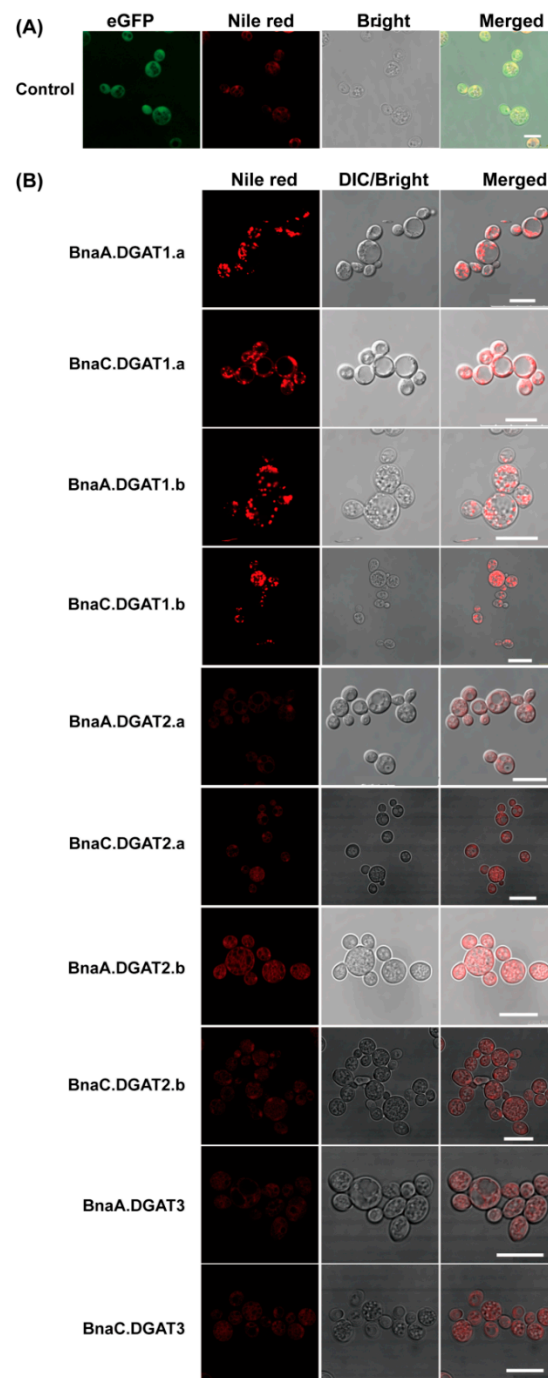


Figure 4. Oil bodies in *S. cerevisiae* H1246 expressing *BnaDGATs* by Nile red staining. **(A)** Negative control. Yeast H1246 expressing *eGFP*; **(B)** Yeast H1246 expressing different *BnaDGATs*. Oil droplets were observed in yeast H1246 expressing *BnaDGAT1s* but were not detectable and/or were very weak in yeast H1246 expressing *BnaDGAT2s* and *BnaDGAT3s*. Bar = 10 μm .

2.7. Fatty Acid Profiles in Yeast H1246 and *INVSc1* Expressing *BnaDGATs*

In this study, the fatty acids in *S. cerevisiae* H1246 and *INVSc1* (*MATa his3 Δ 1 leu2 trp1-289 ura3-52/MAT α his3 Δ 1 leu2 trp1-289 ura3-52*) expressing *BnaDGATs* were quantitatively analyzed by GC–MS to evaluate the effect of *BnaDGATs* on the accumulation of fatty acids in *B. napus* (Figure 5). As shown in Figure 5A, in H1246, the expression of *BnaDGAT1s* resulted in a slight accumulation of C10:0 and C12:0 fatty acids and a significant accumulation of C14:0, C14:1, C16:0, C16:1n7, C18:0 and C18:1n9 fatty acids and increased the content of total fatty acids by one–two times but significantly decreased the content of

C18:1n7 fatty acids. The expression of *BnaDGAT2s* and *BnaDGAT3s* promoted the accumulation of both C14:0 and C14:1 fatty acids. As shown in Figure 5B, in INVSc1, the expression of *BnaDGAT1s* resulted in the significant accumulation of C10:0, C12:0, C14:0, C14:1, C16:0, C16:1n7 and C18:0 and increased the total fatty acid content by approximately 0.23- to 1-fold; the expression of *BnaA.DGAT2.a*, *BnaC.DGAT2.a*, *BnaA.DGAT2.b*, *BnaA.DGAT3* or *BnaC.DGAT3* resulted in the accumulation of C10:0, C14:0 and C14:1. By comparing the effects of *BnaDGATs* on fatty acid accumulation in yeast H1246 and INVSc1, it was found that the expression of *BnaDGAT1s* could promote the accumulation of C10:0, C12:0, C14:0, C14:1, C16:0, C16:1n7, C18:0 and total fatty acids, while the expression of *BnaDGAT2s* and *BnaDGAT3s* could not promote the accumulation of total fatty acids in H1246 and INVSc1.

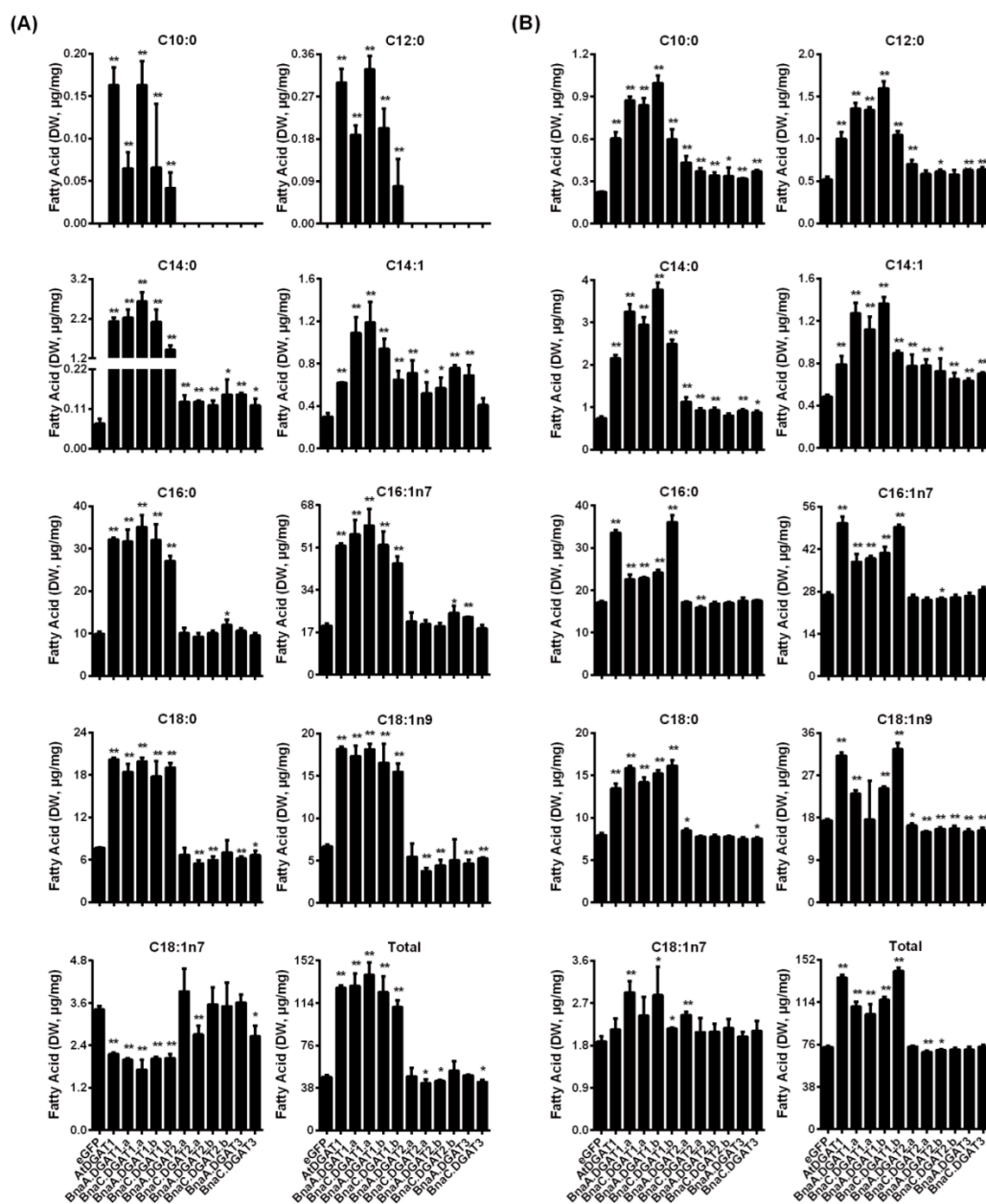


Figure 5. Analysis of the fatty acid compositions and content in yeast H1246 and INVSc1 expressing different *BnaDGATs*. (A) Yeast H1246; (B) Yeast INVSc1. Yeast expressing *eGFP* was the negative control, and that expressing *AtDGAT1* was the positive control. Data represent averages of three replicates \pm SD. Statistical analysis was carried out by Student's *t* test. Asterisks indicate the fatty acids with a significant difference from those in the negative control (* $p < 0.05$; ** $p < 0.01$).

2.8. Transcriptomic and qRT-PCR Analysis of *BnaDGATs* in Different Tissues

The transcriptomic expression data of the *BnaDGAT* gene family from the different tissues of *B. napus* were obtained from BnTIR (<http://yanglab.hzau.edu.cn/BnTIR> (accessed on 10 November 2021)) [60] and BrassicaEDB (<https://brassica.biodb.org/> (accessed on 10 November 2021)) [61]. The extracted data from BnTIR and BrassicaEDB were normalized by $\log_2(\text{TPM})$ and $\log_2(\text{FPKM})$, respectively, and the heatmaps were generated by TBtools (Figure 6). The results showed that the expression patterns of the three *BnaDGAT* gene families were different among diverse tissues. Every homologous pair of *BnaA.DGAT1.a* and *BnaC.DGAT1.a*, *BnaA.DGAT1.b* and *BnaC.DGAT1.b*, *BnaA.DGAT2.a* and *BnaC.DGAT2.a*, *BnaA.DGAT2.b* and *BnaC.DGAT2.b*, and *BnaA.DGAT3* and *BnaC.DGAT3* shared a similar expression pattern. The expression levels of *BnaA.DGAT2.b* and *BnaC.DGAT2.b* were lower than those of other *BnaDGATs* in most detected tissues, while the expression levels of *BnaA.DGAT3* and *BnaC.DGAT3* were higher than those of other *BnaDGATs* in most detected tissues. The expression levels of *BnaA.DGAT1.a* and *BnaC.DGAT1.a* in seeds and embryos gradually increased during seed and embryo development. The expression levels of *BnaA.DGAT1.b* and *BnaC.DGAT1.b* in seeds first gradually increased and then gradually decreased during seed development. The expression levels of *BnaA.DGAT2.a* and *BnaC.DGAT2.a* in seeds, silique walls and embryos first gradually increased and then gradually decreased during the development of seeds, silique walls and embryos. In particular, *BnaA.DGAT1.b* and *BnaC.DGAT1.b* were highly expressed in anthers and stamens.

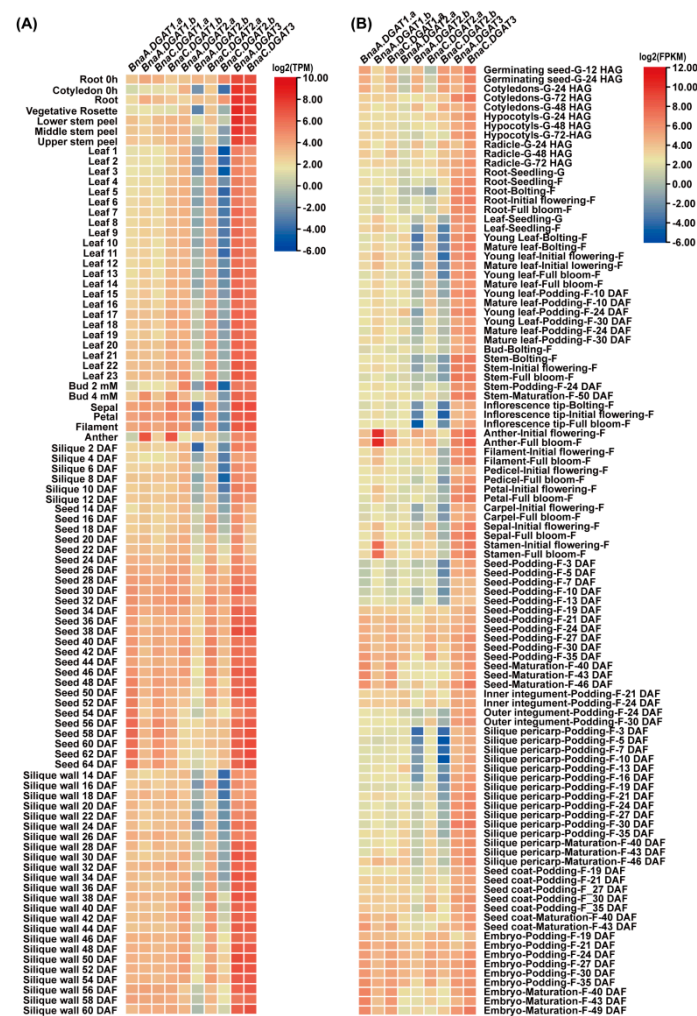


Figure 6. Transcriptomic analysis of *BnaDGATs* in different tissues. (A) The analysis based on BnTIR; (B) The analysis based on BrassicaEDB. RNA-Seq datasets of different tissues at diverse stages of

development were obtained from BnTIR (<http://yanglab.hzau.edu.cn/BnTIR> (accessed on 10 November 2021)) [60] and BrassicaEDB (<https://brassica.biodb.org/> (accessed on 10 November 2021)) [61]. The extracted data from BnTIR and BrassicaEDB were normalized by \log_2 (TPM) and \log_2 (FPKM), respectively, and the heatmaps were generated by TBtools [62].

2.9. Expression Analysis of *BnaDGATs* under Different Stresses

Six-week-old *B. napus* seedlings were used to investigate the expression patterns of *BnaDGATs* in roots, stems and leaves under abiotic stresses, including P starvation, low N, drought and salinity, by qRT-PCR.

Under P starvation, compared with mock, the expression levels of *BnaDGAT1s*, *BnaA.DGAT2.b* and *BnaC.DGAT2.b* in roots, stems and leaves were lower; the expression patterns of *BnaA.DGAT2.a* and *BnaC.DGAT2.a* in roots, stems and leaves were not changed significantly; the expression levels of two *BnaA.DGAT3s* in leaves were decreased, while their expression levels in roots and stems were not changed significantly (Figure 7).

During low N, compared with mock, the expression patterns of four *BnaDGAT1s* in stems and leaves and *BnaA.DGAT1.b* in roots were not changed, while the expression levels of *BnaA.DGAT1.a* and *BnaC.DGAT1.a* in roots were lower. For *BnaDGAT2s*, the expression patterns of *BnaA.DGAT2.a* and *BnaC.DGAT1.a* in roots and stems under low N were not changed, while their expression levels in leaves were lower; the expression levels of *BnaA.DGAT2.b* in leaves and stems were lower, while its expression levels in roots were higher; the expression levels of *BnaC.DGAT2.b* in stems were lower, while its expression levels in leaves and roots were higher. For the two *BnaDGAT3s*, their expression patterns in roots and stems were quite consistent with those in mock, while their expression levels in leaves decreased at the late stages of low N treatment (Figure 7).

During salt stress, compared with mock, the expression levels of four *BnaDGAT1s* in the stems were higher, while their expression levels in roots were lower. For *BnaDGAT2s*, the expression levels of *BnaA.DGAT2.a* and *BnaC.DGAT2.a* in roots, stems and leaves were higher; the expression levels of *BnaA.DGAT2.b* in leaves and stems were lower, while its expression levels in roots were higher; the expression levels of *BnaC.DGAT2.b* in stems were lower, but its expression levels in roots were higher. For *BnaDGAT3s*, the expression levels of *BnaA.DGAT3* in stems and leaves and *BnaC.DGAT3* in roots, stems and leaves were lower than those in mock with 12–48 h stress (Figure 7).

During drought stress, compared with mock, the expression levels of four *BnaDGAT1s* in leaves at 12 h of treatment and *BnaC.DGAT1.a*, *BnaA.DGAT1.b* and *BnaC.DGAT1.b* in roots at 48 h of treatment were higher, while the expression patterns of *BnaA.DGAT1.a* and *BnaC.DGAT1.a* in stems were quite consistent. For *BnaDGAT2s*, the expression levels of *BnaA.DGAT2.a* and *BnaC.DGAT2.a* in stems and leaves were higher; the expression levels of *BnaA.DGAT2.b* in leaves and stems were lower, while its expression levels in roots were higher; the expression patterns of *BnaC.DGAT2.b* in leaves and stems were quite consistent with those in mock, while its expression levels in roots were higher than those in mock. For *BnaDGAT3s*, the expression levels of *BnaA.DGAT3* in stems and roots and *BnaC.DGAT3* in roots were higher than those in mock, while the expression levels of *BnaC.DGAT3* in leaves treated for 12–48 h were quite low (Figure 7).

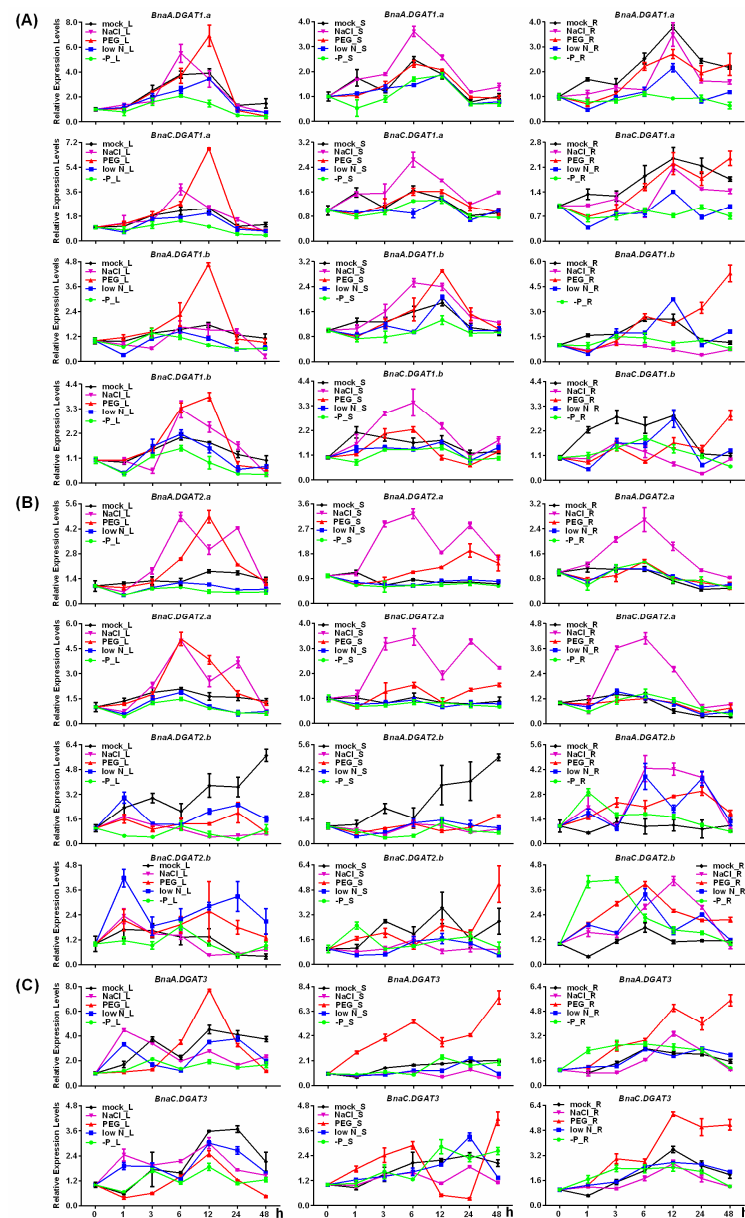


Figure 7. qRT-PCR analyses of different *BnaDGATs* under different stresses. (A) qRT-PCR analyses of *BnaDGAT1s* under different stresses; (B) qRT-PCR analyses of *BnaDGAT2s* under different stresses; (C) qRT-PCR analyses of *BnaDGAT3s* under different stresses. For dehydration and salt stress treatments, six-week-old seedlings of *B. napus* were grown hydroponically in solution containing 15% (*w/v*) PEG6000 and 150 mM NaCl plus 1/2 Hoagland solution. In the Pi-deficient treatment (-P), KH_2PO_4 in 1/2 Hoagland solution was replaced by equimolar amounts of KCl. In the low nitrogen treatment (low N), KNO_3 in 1/2 Hoagland solution was replaced by equimolar amounts of KCl. Seedlings growing in 1/2 Hoagland solution for various periods of time were used as the mock. Tissues at 0 h, 1 h, 3 h, 6 h, 12 h, 24 h and 48 h were sampled. *BnaACT7* was used as an internal control. The expression level of each gene at 0 h in leaves (L), stems (S) and roots (R) was arbitrarily set as 1. The data represent averages of three replicates \pm SD.

2.10. Analysis of Fatty Acids in *B. napus* Seedlings under P Starvation, Low N, Drought and Salinity Stresses

Under the stresses of P starvation, low N, drought and salinity, the contents of fatty acids in *B. napus* roots, stems and leaves were measured by GC-MS (Figure 8).

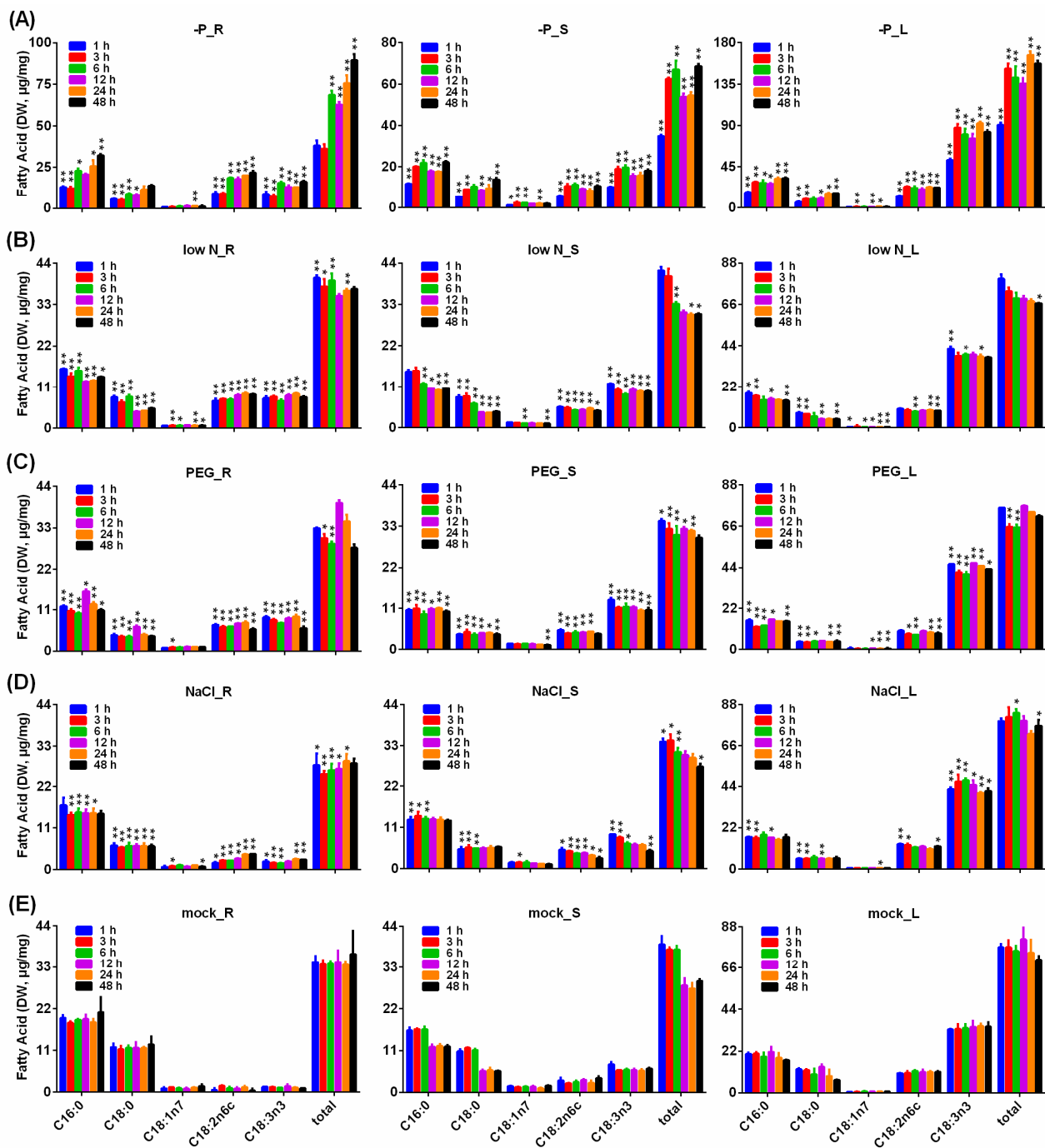


Figure 8. Main fatty acid content in roots, stems and leaves under abiotic stresses. (A) Pi-deficient treatment (-P); (B) Low nitrogen treatment (low N). (C) Dehydration treatment (PEG); (D) Salt treatment (NaCl); (E) Mock. For dehydration and salt stress treatments, six-week-old seedlings of *B. napus* were grown hydroponically in solution containing 15% (*w/v*) PEG6000 and 150 mM NaCl plus 1/2 Hoagland solution. In the Pi-deficient treatment, KH_2PO_4 in 1/2 Hoagland solution was replaced by equimolar amounts of KCl. In the low nitrogen treatment, KNO_3 in 1/2 Hoagland solution was replaced by equimolar amounts of KCl. Seedlings grown in 1/2 Hoagland solution for various periods of time were used as the mock. The FA content was quantified by GC–MS with heptadecanoic acid (C17:0) as an internal standard. The data represent averages of three replicates \pm SD. Asterisks indicate the fatty acid content with a significant difference from those in the mock (* $p < 0.05$; ** $p < 0.01$).

Under P starvation, compared with mock, the content of total fatty acids in roots at 6 h to 48 h, in stems at 3 h to 48 h and in leaves at 1 h to 48 h significantly increased, as well as the content of C18:2n6c and C18:3n3 in roots, stems and leaves at 1 h to 48 h; the content of 16:0 decreased in roots at 1 h and 3 h and in stems and in leaves at 1 h, whereas it increased in roots at 6 h, 24 h and 48 h and in stems and in leaves at 3 h to 48 h; the content of 18:0 decreased in roots at 1 h to 12 h, in stems at 1 h and 3 h and in leaves at 1 h, 3 h and 12 h, whereas it increased in stems at 12 h to 48 h and in leaves at 24 h and 48 h; the content of 18:1n7 decreased in stems at 1 h but increased in roots at 24 h, in stems at 3 h, 6 h and 24 h and in leaves at 3 h, 12 h and 24 h (Figure 8A).

Under low N stress, compared with mock, the accumulation of total fatty acids was promoted in roots at 1 h to 6 h and 24 h and in stems at 24 h and 48 h but inhibited in stems at 6 h and in leaves at 48 h; the content of 16:0 decreased in roots at 1 h to 48 h, in stems at 6 h to 48 h and in leaves at 1 h, 3 h, 12 h and 48 h; the content of 18:0 decreased in roots and stems at 1 h to 48 h and in leaves at 1 h, 3 h, 12 h and 48 h; the content of 18:1n7 decreased in roots at 3 h, 6 h, 24 h and 48 h, in stems at 6 h and 48 h and in leaves at 1 h and 6 h to 48 h; the accumulation of C18:2n6c increased in roots and stems at 1 h to 48 h but decreased in leaves at 6 h, 24 h and 48 h; the content of C18:3n3 increased in roots and stems at 1 h to 48 h and in leaves at 1 h, 6 h and 48 h (Figure 8B).

Under drought stress, compared with mock, the accumulation of total fatty acids was reduced in roots and leaves at 3 h and 6 h and in stems at 1 h to 6 h, while its accumulation in stems at 12 h and 24 h was elevated; the accumulation of 16:0 and 18:0 in roots and stems at 1 h to 48 h and in leaves at 1 h to 12 h and 48 h was reduced, as well as the accumulation of 18:1n7 in roots at 3 h, in stems at 48 h and in leaves at 12 h to 48 h; the accumulation of C18:3n3 in roots, stems and leaves at 1 h to 48 h was increased, as well as the content of C18:2n6c in roots at 1 h to 48 h and in stems at 1 h to 24 h, while the content of C18:2n6c in leaves at 3 h, 6 h, 24 h and 48 h was reduced (Figure 8C).

Under salt stress, compared with mock, the accumulation of total fatty acids was reduced in roots at 1 h to 24 h and in stems at 1 h to 6 h and 48 h, while its accumulation was elevated in leaves at 6 h and 48 h; the content of 16:0 was reduced in roots at 3 h to 24 h, in stems at 1 h to 6 h and in leaves at 1 h, 3 h and 12 h, as well as the content of 18:0 in roots at 1 h to 48 h, in stems at 1 h to 6 h and in leaves at 1 h, 3 h and 12 h; the accumulation of C18:2n6c was increased in roots and stems at 1 h to 48 h and in leaves at 1 h, 3 h and 48 h, as well as the accumulation of C18:3n3 in roots at 1 h to 6 h, 24 h and 48 h, in stems at 1 h to 6 h and 48 h and in leaves at 1 h to 48 h. (Figure 8D).

2.11. *Cis-Elements in BnaDGAT Promoters and Transcription Factors and miRNA Regulating BnaDGATs*

To gain more insights into the potential function and regulatory mechanism of ten *BnaDGATs*, we analyzed the *cis*-regulatory elements in their putative promoters by using the plantCARE database. The putative promoters of ten *BnaDGATs* were cloned as 1759 bp, 1488 bp, 1657 bp, 836 bp, 775 bp, 2151 bp, 1973 bp, 1660 bp and 1459 bp from ZS11 (Table 2 and Table S6). The putative promoters of three *AtDGATs* were derived from TAIR (Table S9). The *cis*-acting regulatory elements in the 776–1500 bp upstream promoter regions of *BnaDGATs* and *AtDGATs* were displayed (Figure 9 and Table S10).

As the putative promoters of *DGAT1s*, they all shared some light-responsive elements. All $P_{AtDGAT1}$, $P_{BnaA.DGAT1.a}$, $P_{BnaC.DGAT1.a}$, and $P_{BnaC.DGAT1.b}$ shared anaerobic induction elements and gibberellin-responsive elements. $P_{AtDGAT1}$, $P_{BnaA.DGAT1.a}$ and $P_{BnaC.DGAT1.a}$ possessed MeJA-responsive elements and defense and stress-responsive elements. Both $P_{AtDGAT1}$ and $P_{BnaA.DGAT1.a}$ contained a circadian control element. Both $P_{BnaA.DGAT1.b}$ and $P_{BnaC.DGAT1.b}$ had a low-temperature-responsive element. $P_{AtDGAT1}$ contained a drought-inducibility element. $P_{BnaC.DGAT1.a}$ contained an SA-responsive element. $P_{BnaA.DGAT1.a}$ contained two GCN4_motifs and three Skn-1_motifs, which are endosperm-expressive elements. In addition, $P_{BnaA.DGAT1.a}$ contained a seed-specific RY element. There was only one Skn-1_motif in $P_{BnaC.DGAT1.a}$.

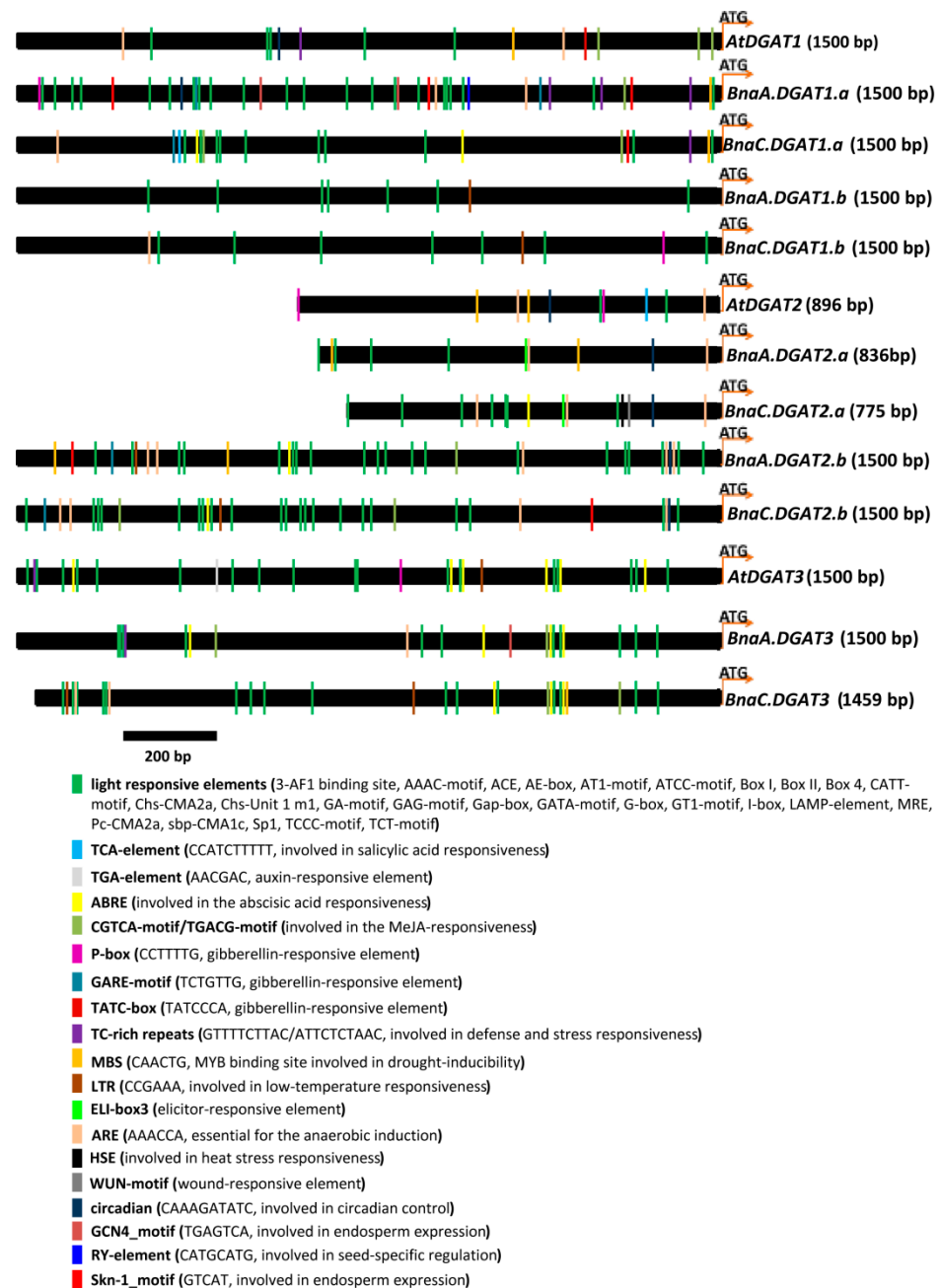


Figure 9. Potential *cis*-acting regulatory elements upstream of the start codons of *BnaDGATs* and *AtDGATs* deduced by PlantCARE. $P_{BnaA.DGAT1.a}$, $P_{BnaC.DGAT1.a}$, $P_{BnaA.DGAT1.b}$, $P_{BnaC.DGAT1.b}$, $P_{BnaA.DGAT2.a}$, $P_{BnaC.DGAT2.a}$, $P_{BnaA.DGAT2.b}$, $P_{BnaC.DGAT2.b}$, $P_{BnaA.DGAT3}$ and $P_{BnaC.DGAT3}$ were cloned from *B. napus* ZS11. $P_{AtDGAT1}$, $P_{AtDGAT2}$ and $P_{AtDGAT3}$ were derived from the Arabidopsis database (<https://www.arabidopsis.org> (accessed on 25 March 2020)). $P_{BnaC.DGAT1.b}$ was extracted from the ZS11 genome database (https://www.ncbi.nlm.nih.gov/assembly/GCF_000686985.2/ (accessed on 20 September 2021)). Black bar = 200 bp.

The putative promoters of *AtDGAT2* and *BnaDGAT2s* also contained some light-responsive elements, anaerobic induction elements and circadian control elements. $P_{AtDGAT2}$, $P_{BnaA.DGAT2.a}$ and $P_{BnaC.DGAT2.a}$ shared a drought-responsive element. $P_{AtDGAT2}$, $P_{BnaA.DGAT2.b}$ and $P_{BnaC.DGAT2.b}$ contained gibberellin-responsive elements. $P_{BnaC.DGAT2.a}$, $P_{BnaA.DGAT2.b}$ and $P_{BnaC.DGAT2.b}$ shared a Skn-1_motif and an ABA-responsive element. Both $P_{BnaA.DGAT2.b}$ and $P_{BnaC.DGAT2.b}$ had a low-temperature-responsive element. Both $P_{BnaA.DGAT2.a}$ and $P_{BnaC.DGAT2.a}$ shared an elicitor-responsive element. Both $P_{BnaA.DGAT2.b}$ and $P_{BnaC.DGAT2.b}$

contained one MeJA-responsive element. $P_{AtDGAT2}$ contained an auxin-responsive element and an SA-responsive element. $P_{BnaC.DGAT2.a}$ contained a heat-stress-responsive element and a wound-responsive element.

$P_{AtDGAT3}$, $P_{BnaA.DGAT3}$ and $P_{BnaC.DGAT3}$, also contained some light-responsive elements and ABA-responsive elements. Both $P_{BnaA.DGAT3}$ and $P_{BnaC.DGAT3}$ contained MeJA-responsive elements. Both $P_{AtDGAT3}$ and $P_{BnaA.DGAT3}$ shared a defense- and stress-responsive element. Both $P_{AtDGAT3}$ and $P_{BnaC.DGAT3}$ contained low-temperature-responsive elements. $P_{AtDGAT3}$ contained a gibberellin-responsive element and an auxin-responsive element. $P_{BnaA.DGAT3}$ contained an endosperm expression element and an anaerobic induction element. $P_{BnaC.DGAT3}$ contained a drought-responsive element.

Transcription factors (TFs) regulate the precise initiation of gene transcription by binding the *cis*-acting elements of gene promoters. Therefore, we identified the target TFs putatively regulating the expression of *BnaDGATs* using the PlantRegMap server, and a total of 209 relationships were identified (Table S11). Three *BnaDGAT* gene families may be regulated by different TFs, such as the B3 family, dehydration-responsive element-binding protein (DREB), GATA, ethylene response factor (ERF), WRKY family, MYB and bZIP family, indicating that these TFs regulate plant development and stress responses.

miRNAs have been widely shown to play an important role at the transcriptional and posttranscriptional levels in regulating gene expression under stress [63,64]. Therefore, we predicted that the *bna*-miRNAs would target *BnaDGATs* using the psRNATarget website (www.zhaolab.org/psRNATarget/ (accessed on 25 November 2021)). The results showed that four miRNAs (*bna*-miR2111a-3p, *bna*-miR390a, *bna*-miR390b and *bna*-miR390c) only targeted *BnaA.DGAT2.b* and *BnaC.DGAT2.b* and that no miRNAs targeted *BnaDGAT1s* or *BnaDGAT3s* (Table S12). For *B. rapa*, *bra*-miR9562-5p was predicted to target *BraDGAT1s* (*BraA07g001370.3C* and *BraA09g011830.3C*), *bra*-miR2111a-3p to target one *BraDGAT2* (*BraA03g045590.3C*) and *bra*-miR5721 to target *BraDGAT2s* (*BraA01g022340.3C* and *BraA03g045590.3C*) (Table S12). For *B. oleracea*, no miRNA was predicted to target the *BolDGATs*. In addition, six miRNAs (*ath*-miR3434-5p, *ath*-miR5020b, *ath*-miR5629, *ath*-miR5633, *ath*-miR5654-3p and *ath*-miR858a) were predicted to target *AtDGAT1*, six miRNAs (*ath*-miR2936, *ath*-miR390a-5p, *ath*-miR390b-5p, *ath*-miR5641, *ath*-miR835-5p and *ath*-miR847) to target *AtDGAT2* and two miRNAs (*ath*-miR847 and *ath*-miR4221) to target *AtDGAT3* (Table S12).

3. Discussion

B. napus is an allotetraploid (AACC) crop that originated from the hybridization of two diploid progenitors, *B. rapa* (AA) and *B. oleracea* (CC) [51,52]. In this study, ten *BnaDGATs* were cloned and identified from *B. napus* and grouped into three subfamilies—*BnaDGAT1*, *BnaDGAT2* and *BnaDGAT3*—based on their homology. Systematic analyses of chromosome location, gene synteny, physicochemical properties, phylogenetic tree, exon/intron gene structure, conserved domain and motif compositions, TMDs and the distribution of *cis*-elements in the promoters were performed. The functions of *BnaDGATs* were detected in yeast H1246 and INVSc1. Moreover, qRT-PCR and prepublished RNA-seq data were analyzed to determine the expression patterns of *BnaDGATs*. These results provide an extensive evaluation of *BnaDGATs* and a useful foundation for dissecting the functions of *BnaDGATs* in biochemical and physiological processes.

3.1. Gene Duplication and Functional Diversification of DGAT Family Members

The phylogenetic tree showed that *BnaDGATs* were grouped into three well-supported clades: the DGAT1 subfamily, the DGAT2 subfamily and the DGAT3 subfamily (Figure 2A). Identity analysis showed that the three DGAT subfamilies shared very low identity with each other subfamily (Table S8). Gene synteny analysis showed that there was no gene synteny among the three DGAT subfamilies (Figure 1). The analysis of gene structures revealed distinct differences among the three *DGAT* subfamilies in exon/intron gene structure (Figures 2B and S2B). Conserved domain and motif analyses showed that the

three DGAT subfamilies had different conserved domains and motifs (Figures 2C and S3B). Each DGAT1 was predicted to harbor seven to ten putative TMDs, one to four putative TMDs were detected in most DGAT2s and there were no putative TMDs in any of the examined DGAT3s (Figure 3 and Table S7). The expression patterns of the three *Bna*DGAT gene families were different among diverse tissues (Figure 6). All of these results showed that the DGAT1, DGAT2 and DGAT3 gene subfamilies showed apparent differences and indicated that they are divergent genes and may have a distinct origin, consistent with what is described in soybeans [65] and upland cotton [25]. In addition, the results of this study showed that three *Bna*DGAT gene subfamilies were frequently duplicated during the speciation and evolution of *B. oleracea*, *B. rapa* and *B. napus* and suggested that *B. napus* inherited and retained all the DGAT genes of *B. rapa* and *B. oleracea* (Figures 1 and S1), consistent with what is described in tetraploid cotton [25].

3.2. Role of *Bna*DGATs in Oil Biosynthesis

DGAT1 has been functionally confirmed in oil biosynthesis in Arabidopsis, soybean, oilseed rape, and so on [3]. Expression analysis revealed that DGAT1 was abundantly expressed in the developing embryos in several oilseed crops, and its transcript level was correlated with oil accumulation in developing seeds [49]. Analysis of the putative promoters showed that $P_{BnaA.DGAT1.a}$ contained two GCN4 motifs (endosperm expressive elements), three Skn-1 motifs (endosperm expressive elements) and one seed-specific RY-element and that $P_{BnaC.DGAT1.a}$ possessed one Skn-1 motif (Figure 9). In this study, the expression levels of *BnaA.DGAT1.a* and *BnaC.DGAT1.a* in seeds and embryos gradually increased during seed and embryo development (Figure 6), which corresponded with the rapid oil accumulation stage in canola seeds, indicating that *BnaA.DGAT1.a* and *BnaC.DGAT1.a* were important in TAG biosynthesis in canola seeds. The expression levels of *BnaA.DGAT1.b* and *BnaC.DGAT1.b* in seeds first gradually increased and then gradually decreased during seed development, and the expression levels of *BnaA.DGAT2.a* and *BnaC.DGAT2.a* in seeds, silique walls and embryos first gradually increased and then gradually decreased during the development of seeds, silique walls and embryos (Figure 6), which implied that *BnaA.DGAT1.b*, *BnaC.DGAT1.b*, *BnaA.DGAT2.a* and *BnaC.DGAT2.a* may also play an important role in TAG biosynthesis in canola seeds. Moreover, there were high expression levels of *BnaA.DGAT1.b* and *BnaC.DGAT1.b* in the anthers and stamens of canola, indicating that *Bna*DGAT1 might be involved in the reproductive development of oilseed rape.

It was reported that tung tree TAG production via DGAT1 and DGAT2 occurs in a distinct ER subdomain and that DGAT1 and DGAT2 differ in substrate preference [9]. In this study, *Bna*DGAT1s and *Bna*DGAT2s were predicted to harbor putative TMDs and to be located in the ER (Table 2 and Figure 3). Then, we overexpressed *Bna*DGAT1s and *Bna*DGAT2s in yeast H1246 and INVSc1 and found that only four *Bna*DGAT1s were able to re-establish TAG synthesis in yeast H1246 (Figure 4) and could promote the accumulation of total fatty acids in H1246 and INVSc1 (Figure 5). In previous studies, 16:0-CoA and 18:1-CoA were the best substrates of *BnaA.DGAT1.a*, *BnaC.DGAT1.a* and *BnaC.DGAT1.b* with [¹⁴C]glycerol labelled di-6:0-DAG as an acyl acceptor and with either 16:0-CoA, 18:0-CoA, 18:1-CoA, 18:2-CoA, 18:3-CoA or 22:1-CoA as acyl donors [45], and the preference of four *Bna*DGAT1s for 16:0-CoA was four–seven times as high as that for 18:1-CoA when the ratio of 18:1-CoA to 16:0-CoA was 1:1, while their preference for 18:1-CoA was two–five times as high as that for 16:0-CoA when the ratio of 18:1-CoA to 16:0-CoA was 3:1 [20]. However, the N-terminus *Bn*DGAT1₍₁₋₁₁₆₎ of *Bn*DGAT1 (AF164434, *BnaA.DGAT1.b*) binds to 22:1*cis*^{Δ13}-CoA more strongly than 18:1*cis*^{Δ9}-CoA [66], and purified *BnaC.DGAT1.a* exhibited substrate preference for 18:3-CoA > 18:1-CoA = 16:0-CoA > 18:2-CoA > 18:0-CoA [67]. Here, *Bna*DGAT1s were found to prefer C16 (C16:0 and C16:1n7) and C18 (C18:0 and C18:1n9) as substrates instead of C10, C12 and C14 in yeast H1246 and INVSc1 (Figure 5). DGAT2s were previously found to prefer unusual or polyunsaturated fatty acids [8,9,43,44,68–70]. Unusual or polyunsaturated fatty acids were not detected in H1246

and INVSc1 in this study, which may be because saturated and monounsaturated fatty acids are the main components of the fatty acids in *S. cerevisiae* [71].

Some studies have focused on the role of DGAT3 in TAG biosynthesis [10,25,46,47,72]. In this study, almost all DGAT3 homologues were found to share the TRX_Fd_family domain (Figure 2C). To date, AtDGAT3 and CsDGAT3 have been confirmed as metalloproteins involved in TAG biosynthesis in plants [46,72]. DGAT3 homologues were not found in mossy or algal species [73], indicating that they may have arisen during plant evolution. The expression levels of *BnaDGAT3s* were significantly higher than those of *BnaDGAT1s* and *BnaDGAT2s* during canola seed development (Figure 6), consistent with what is described in upland cotton and soybean [65,74]. In this study, overexpressing *BnaDGAT3s* could not restore TAG synthesis in yeast H1246 and did not promote the accumulation of fatty acids (Figures 4 and 5). Therefore, the function of *BnaDGAT3s* in synthesizing TAGs needs further testing using oilseed rape or other protein expression systems.

3.3. The Response of *BnaDGATs* to Abiotic Stresses

Phosphorus starvation can increase the accumulation of oils in most microalgae [75–80] as well as in the vegetative tissues of plants, such as *Arabidopsis*, tomato, tobacco and barnyard grass (*Echinochloa crusgalli*) [81,82]. In this study, we found that the accumulation of total fatty acids was greatly promoted (Figure 8A), but the expression levels of *BnaDGAT1s*, *BnaDGAT2s* and *BnaDGAT3s* were not enhanced in the roots, stems and leaves of *B. napus* seedlings under P starvation (Figure 7). In *Arabidopsis*, the expression of genes involved in TAG synthesis, such as *AtDGAT1*, *AtDGAT2*, *AtPDAT1*, *AROD1*, *AtLPCAT2*, *AtBCCP2* and *PDH-E1a*, was not increased under P starvation [81,82]. The above studies showed that the expression levels of *DGAT1s* were not directly related to the increase in TAG accumulation under P starvation. In previous studies, a self-inhibiting motif in the N-terminal region of *BnaDGAT1* bound PA and shifted *BnaDGAT1* to a higher activity state [83,84]; PLDZ2 (phospholipase D Z2) degraded phospholipids into PA and was induced by P starvation [85,86]. SnRK1 (Snf1-related kinase 1) inhibited *DGAT1* activities by phosphorylating S/T in the SnRK1 targeting motif [23,52,84], and the activity of *Arabidopsis* SnRK1 was reduced and its catalytic subunit AKIN11 was degraded under P starvation [87]. Therefore, the enhancement of TAG accumulation may be related to the higher activities of *DGAT1s* regulated by the increase in PA and the decrease in SnRK1 activity under P starvation. In addition to TAG, P starvation can also promote the accumulation of DAG, MGDG, DGDG and SQDG by inducing the expression of *NPC4*, *NPC5*, *PLDZ2*, *PAH1*, *PAH2*, *MGD2*, *MGD3*, *DGD1*, *DGD2*, *SQD1* and *SQD2* in *Arabidopsis* seedlings [81,82]. This result suggested that the increase in total fatty acids is a consequence of the accumulation of TAG, DAG, MGDG, DGDG and SQDG in *B. napus* seedlings under P starvation, which may be caused by gene expression changes similar to those in *Arabidopsis*.

Many studies have shown that most microalgae can accumulate high levels of oil under N starvation [75,88–94]. For plants, N and C are closely coordinated to affect chloroplast lipid metabolism and TAG content [36,95–97]. This study found that low N (5 mM) promoted the accumulation of total fatty acids in roots at 1 h to 6 h and 24 h and in stems at 24 h and 48 h, but inhibited the accumulation of total fatty acids in stems at 6 h and in leaves at 48 h (Figure 8B). In previous reports, low N (0.1 mM and 0.65 mM) promoted TAG accumulation, especially 0.1 mM N with 50 mM sucrose, by inducing the expression of *AtDGAT1*, *AtDGAT2*, *AtPDAT1* and *AtOLEOSIN1* in *Arabidopsis* seedlings [36,96]. In this study, low N (5 mM) did not induce the expression of four *BnaDGAT1s*, *BnaA.DGAT2.a*, *BnaC.DGAT2.a* and two *BnaDGAT3s* in roots, stems and leaves; *BnaA.DGAT2.b* in leaves and stems and *BnaC.DGAT2.b* in stems but promoted the expression of *BnaA.DGAT2.b* in roots and *BnaC.DGAT2.b* in leaves and roots (Figure 7). In previous studies, *Arabidopsis* seedlings were cultured under low N (0.1 mM) using Murashige and Skoog (MS) solid medium, while *B. napus* seedlings were cultured under low N (5 mM) in this study using Hoagland solution without carbon sources. In normal 1/2 Hoagland solution, the nitrogen content

was 7.5 mM. Therefore, it may not be sufficient to induce the expression of *BnaDGATs* in *B. napus* under 5 mM N (50 times that under 0.1 mM).

In this study, the accumulation of total fatty acids in roots and leaves at 3 h and 6 h and in stems at 1 h to 6 h was reduced but was promoted in stems at 12 h and 24 h using 15% PEG for stress treatment (Figure 8C). Previous studies showed that drought stress reduced phospholipids (PC, PE, PG), glycolipids (MGDG and DGDG) and total fatty acids in *B. napus* and increased neutral lipids (mainly TAG) [98–101], which is consistent with maize [102], soybean [103] and cotton [104]. Therefore, the changes in total fatty acids in the roots, stems and leaves of *B. napus* seedlings under drought stress were the combined result of a decrease in phospholipids and an increase in neutral lipids. In this study, drought stress for 24 h increased the expression levels of four *BnaDGAT1s* in leaves, *BnaA.DGAT2.a* and *BnaC.DGAT2.a* in stems and leaves; *BnaA.DGAT2.b* and *BnaC.DGAT2.b* in roots; *BnaA.DGAT3* in stems and roots and *BnaC.DGAT3* in roots, but decreased the expression levels of *BnaA.DGAT2.b* in leaves and stems and *BnaC.DGAT3* in leaves (Figure 7). A previous study showed that the expression of *AtDGAT1* was promoted by ABI4 and ABI5 under drought stress [38]. Therefore, it is necessary to further test whether ABI4 and ABI5 participate in the regulation of *BnaDGAT* expression in *B. napus* under drought stress. Furthermore, drought-inducible elements (MBS) were found in the potential promoters of *BnaA.DGAT2.a*, *BnaA.DGAT2.b*, *BnaC.DGAT2.b*, *BnaA.DGAT3* and *BnaC.DGAT3* (Figure 9 and Table S10). In *Arabidopsis*, MBS is generally present in the promoter of drought-inducible genes and bound by AtMYB2 in response to drought stress [105–107]. The expression of AtMYB2 was induced by drought, salt or ABA treatment in *Arabidopsis* seedlings [105]. Therefore, the expression levels of *BnaA.DGAT2.a*, *BnaA.DGAT2.b*, *BnaC.DGAT2.b*, *BnaA.DGAT3* and *BnaC.DGAT3* may be regulated by BnaMYB2 under drought stress, which needs to be further tested.

For most microalgae, the appropriate salinity (20–40 g/L, i.e., 340–680 mM) can increase the accumulation of lipids, while lipid accumulation will be negatively affected when the salinity is excessive [75]. In *Arabidopsis*, TAG accumulation and the expression of *DGAT1* were promoted by enhancing the expression of *ABI4* and *ABI5* under salt stress (100 mM NaCl) [38]. In this study, it was found that the accumulation of total fatty acids was reduced in roots at 1 h to 24 h and in stems at 1 h to 6 h and 48 h, while it was elevated in leaves at 6 h and 48 h under salt stress (150 mM NaCl; Figure 8D). Moreover, the expression levels of four *BnaDGAT1s* in stems; *BnaA.DGAT2.a* and *BnaC.DGAT2.a* in roots, stems and leaves and *BnaA.DGAT2.b* in roots were increased, but the expression levels of four *BnaDGAT1s* in roots; *BnaA.DGAT2.b* in leaves and stems; *BnaC.DGAT2.b* in stems; *BnaA.DGAT3* in stems and leaves and *BnaC.DGAT3* in roots, stems and leaves at 12–48 h of stress decreased (Figure 7). Therefore, it is necessary to further test and explore the relationship between the accumulation of fatty acids and the expression of *BnaDGATs* in *B. napus* under salt stress.

4. Materials and Methods

4.1. Identification of DGAT Family Members in *B. napus* and in Other Plants

To identify candidate DGAT family members in *B. napus*, the CDS and peptide sequences of the three *AtDGATs* from the *A. thaliana* genome database (<http://www.arabidopsis.org/> (accessed on 25 March 2020)) with corresponding Gene IDs (At2G19450, At3G51520 and At1G48300) were retrieved and used as queries to perform BLAST searches in two *B. napus* Genome Databases (BnPIR, <http://cbi.hzau.edu.cn/bnapus> (accessed on 2 March 2021), and GENOSCOPE, <https://www.genoscope.cns.fr/brassicapnapus/> (accessed on 25 March 2020)) with the default parameters. The CDSs and genomic DNAs of *BnaDGATs* were cloned from *B. napus* ZS11 using primers (Table S1), designed according to the nucleotide sequences of *BnaDGATs* retrieved from the two *B. napus* genome databases. The *DGATs* of *B. oleracea*, *B. rapa*, *B. juncea* and *B. nigra* were downloaded from the Brassica Database (BRAD, <http://brassicadb.cn/#/> (accessed on 11 October 2021)). *B. carinata* *DGATs* were derived from the Brassica Genomics Database (BGD,

<http://brassicadb.bio2db.com/> (accessed on 11 October 2021)). DGAT family members in *A. hypogaea*, *G. max*, *R. communis*, *O. sativa*, *Z. mays*, *S. italica*, *M. truncatula*, *B. distachyon* and *J. curcas* were blasted and selected from their corresponding genome databases (Table S2). Then, the theoretical molecular weight (MW) and isoelectric point (pI) were predicted using the ProtParam tool (<https://web.expasy.org/protparam/> (accessed on 22 October 2021)) on the basis of their amino acid sequences. The subcellular location pattern of each BnaDGAT was evaluated via ProtComp v.9.0 in softberry (<http://linux1.softberry.com/> (accessed on 22 October 2021)). Multiple sequence alignments of DGATs of *B. napus*, *B. oleracea* and *B. rapa* were performed based on full-length proteins and full-length CDSs by ClustalW, and their identities were evaluated by Sequence Distances in MegAlign software.

4.2. Chromosomal Location and Gene Synteny Analysis

The detailed chromosome locations of DGATs in *B. napus*, *B. rapa* and *B. oleracea* were acquired from the GFF genome files downloaded from the *B. napus* genomic database (Bn-PIR, <http://cbi.hzau.edu.cn/bnapus> (accessed on 11 October 2021)) and *Brassica* Database (BRAD, <http://brassicadb.cn/#/> (accessed on 11 October 2021)), respectively, and the predicted locations on the chromosomes were mapped by using TBtools software [62], with red-colored gene names indicated as relative positions. Gene synteny analyses of DGATs in *A. thaliana*, *B. oleracea*, *B. rapa*, *B. napus* and *B. nigra* were carried out by using TBtools software [62]. In addition, we calculated the synonymous (Ks), nonsynonymous mutations (Ka) and Ka/Ks ratio at each codon by Tbttools [62]. In addition, the DGAT gene pair duplication time was presumed using the formula $T = Ks/2R$, with R (1.5×10^{-8}) representing neutral substitution per site per year [108].

4.3. Phylogenetic, Gene Structure, Conserved Domain and Motif Analyses

The MUSCLE program in MEGA11 software was used to perform DGAT alignments with amino acid sequences by default parameters, and then the rectangular phylogenetic tree was constructed using the neighbor-joining (NJ) method with 2000 bootstrap replications. The rectangular phylogenetic tree Newick format was saved for constructing the gene structure, conserved domain and motifs. The genomic and coding sequences of DGAT genes were obtained from their corresponding genome databases (Table S2) and rendered in the Gene Structure Display Server (GSDS2.0; <http://gsds.gao-lab.org/> (accessed on 20 October 2021)) [56] to construct their gene structures. Amino acid sequences of DGATs were submitted to the MEME program (Version 5.4.1, <https://meme-suite.org/meme/tools/meme> (accessed on 21 October 2021)) with the maximum motif search set to 20 and other parameters set to default to identify the conserved protein motifs [109]. A functional search of the conserved domains was performed using the Conserved Domain Database (CDD) with Batch CD-Search in NCBI. The conserved motifs and domains were visualized by using TBtools software [62]. The putative transmembrane domains of DGATs were predicted using TMHMM Server v. 2.0 (<https://services.healthtech.dtu.dk/service.php?TMHMM-2.0> (accessed on 10 April 2021)). Multiple sequence alignments of DGATs were performed based on their full-length proteins by ClustalW in MegAlign software and then crested with CLC Sequence Viewer 6.8 software.

4.4. Yeast Expression Vector Construction and Transformation

First, the CDSs of ten *BnaDGATs*, one *AtDGAT1* (as a positive control) and one *eGFP* (as a negative control) were cloned into the entry vector pGWC using the corresponding primers (Table S1) and then recombined into the Gateway vector pYES-DEST52 (Invitrogen). The constructs were introduced into yeast H1246 (*MAT α are1- Δ ::HIS3, are2- Δ ::LEU2, dga1- Δ ::KanMX4, lro1- Δ ::TRP1 ADE2*) [59] and INVSc1 (*MAT α his3 Δ 1 leu2 trp1-289 ura3-52/MAT α his3 Δ 1 leu2 trp1-289 ura3-52*), according to the *Yeast Protocols Handbook* from Clontech Laboratories Inc. (Mountain View, CA, USA) Transformants were selected on synthetic complete medium lacking uracil (SC-ura).

4.5. Nile Red Staining and Microscopy

Lipid droplets in the transformants of yeast H1246 were stained with Nile Red and then visualized on a Leica TCS SP5 (Leica Microsystems, Wetzlar, Germany) laser scanning confocal microscope, as previously described [92].

4.6. Analysis of Fatty Acids in Yeast Transformants and *B. napus* Seedlings by GC–MS

The transformants of yeast H1246 and INVSc1 first cultured with liquid SC-ura medium containing 2% (*w/v*) glucose at 30 °C overnight were then diluted to $OD_{600} = 0.1$ with liquid SC-ura medium containing 2% (*w/v*) galactose and 1% (*w/v*) raffinose and shaken at 30 °C and 250 rpm for 72 h. The yeast cells were harvested by centrifugation and dried at 55 °C, and then the pellets were ground to a fine powder. For *B. napus* seedlings, samples of roots, stems and leaves were also ground to a fine powder under liquid nitrogen and then freeze-dried. For fatty acid extraction, 50 mg of yeast powder or 15 mg of freeze-dried powder of every *B. napus* sample was incubated in 3 mL of 7.5% (*w/v*) KOH in methanol for saponification at 70 °C for 5 h. Then, the pH was adjusted to 2.0 with HCl, and the fatty acid was subjected to methyl-esterification with 2 mL of 14% (*w/v*) boron trifluoride in methanol at 70 °C for 2 h. A phase separation was produced by adding 2 mL of 0.9% (*w/v*) NaCl and 4 mL of hexane. The upper phase was dried under a nitrogen gas flow and resuspended in acetic ether. Analysis of fatty acid methyl esters (FAMES) was performed by GC–MS (GC-QQQ, 7890A-7001B, Agilent Technologies, Santa Clara, CA, USA) equipped with a capillary column (HP-FFAP, 30 mm × 0.25 mm ID, 0.25 µm; Agilent Technologies). Hydrogen was used as the carrier gas at a flow rate of 1.0 mL/min. The injection port, transmission line and ion source temperatures were held at 220 °C, 230 °C and 230 °C, respectively. The temperature of the column oven was programmed from 60 to 180 °C at 10 °C/min, then from 180 to 210 °C at 3 °C/min, and finally from 210 to 220 °C at 5 °C/min and held for 15 min. The FA content was quantified using heptadecanoic acid (C17:0, Sigma, St. Louis, MO, USA) as an internal standard added to samples prior to extraction. All experiments were performed in biological triplicates.

4.7. *B. napus* Seedling Treatments and Sampling

The seedlings of *B. napus* Westar were hydroponically cultured in 1/2 Hoagland solution [110] for six weeks with a 16 h day/8 h night cycle at 23 °C and then were used for the stresses of P starvation (KH_2PO_4 replaced by an equimolar amount of KCl), low N (KNO_3 replaced with an equimolar amount of KCl), drought (15% *w/v* PEG6000) and salinity (150 mM NaCl). Seedlings cultured in normal 1/2 Hoagland solution were used as the control group (mock). Roots, stems and leaves of seedlings were sampled at seven time points: 0 h, 1 h, 3 h, 6 h, 12 h, 24 h and 48 h. The collected samples were immediately dipped in liquid nitrogen and then stored at –80 °C for the relative expression levels of *BnaDGATs* and fatty acid analysis. All experiments were performed in biological triplicates.

4.8. Genomic DNA Extraction, Total RNA Isolation, Primary cDNA Synthesis and qRT–PCR

Genomic DNA of *B. napus* ZS11 was extracted using a method modified from a CTAB-based protocol [111] for cloning genomic DNA of *BnaDGATs*. Total RNA of *B. napus* was extracted using an RNAprep Pure Plant Kit (DP432, TIANGEN BIOTECH Co., Ltd., Beijing, China), and *B. napus* complementary DNA was synthesized using TransScript One-Step gDNA Removal and cDNA Synthesis SuperMix (AT311-03, TransGen Biotech, Beijing, China), according to the manufacturer's instructions. For qRT–PCR, 2 µg of total RNA was first used for the synthesis of first-strand cDNA using oligo(dT)₁₈ as a primer, and then qRT–PCR was performed on a CFX Connect™ Real-Time PCR system (Bio–Rad, Hercules, CA, USA) using EvaGreen 2× qPCR MasterMix (MasterMix-S, Abm, Vancouver, BC, Canada), according to the manufacturer's instructions. The specificity of primers (Table S3) for qRT–PCR was confirmed by separating the products on agarose gels and clone sequencing. *BnaACT7* was used as an internal reference gene, and the relative expression

levels of each *BnaDGAT* to *BnaACT7* in leaves, stems and roots at 0 h were set to 1. All qRT-PCRs were performed in biological triplicates.

4.9. Expression Pattern Analysis Based on RNA-Seq Datasets

The transcript level was calculated based on publicly released data. RNA-Seq datasets of different tissues at diverse stages of development were obtained from BnTIR (<http://yanglab.hzau.edu.cn/BnTIR> (accessed on 10 November 2021)) [60] and BrassicaEDB (<https://brassica.biodb.org/> (accessed on 10 November 2021)) [61]. The extracted data from BnTIR and BrassicaEDB were normalized by $\log_2(\text{TPM})$ and $\log_2(\text{FPKM})$, respectively, and the heatmaps were generated by TBtools [62].

4.10. Analyses of Transcription Factors and miRNAs Targeting *BnaDGATs* and Cis-Acting Elements in *BnaDGAT* Promoters

Transcription factors regulating *BnaDGATs* were predicted using PlantRegMap [112], with *B. napus* as the target. The full-length cDNA sequences of *BnaDGAT* homologues were submitted to the psRNATarget website (<https://www.zhaolab.org/psRNATarget/> (accessed on 25 November 2021)) [113] for a potential miRNA search against the *B. napus* miRNA database. For cis-element analysis, the regions 776–1500 bp upstream of the start codon of *BnaDGATs* and *AtDGATs* were subjected to the plantCARE database (<http://bioinformatics.psb.ugent.be/webtools/plantcare/html/> (accessed on 20 September 2021)) [114] for cis-element searching.

5. Conclusions

In summary, ten *BnaDGATs* were identified and grouped into three different DGAT subfamilies. These *BnaDGATs* are derived from three different ancestors and evolved separately during plant evolution, as proposed by analyzing physicochemical properties, chromosome location, gene synteny, phylogenetic tree, exon/intron gene structure, conserved domain and motif compositions and TMDs. *BnaDGAT1s* possess the ability to introduce the fatty acids C10, C12, C14, C16 and C18 into TAG in *S. cerevisiae* and a higher preference for the fatty acids C16:0, C16:1n7, C18:0 and C18:1n9 than C10:0, C12:0, C14:0, C14:1 and C18:1n7. *BnaDGAT1s* are the main diacylglycerol acyltransferases that synthesize TAGs in *B. napus*. The role of *BnaDGAT2s* and *BnaDGAT3s* in TAG synthesis in *B. napus* needs to be further clarified. Some B3, bZIP, MYB-like transcription factors and other transcription factors involved in the response to light signals may regulate the expression of *BnaDGATs*. P starvation increased fatty acid accumulation in *B. napus* seedlings. The relationships between the expression of *BnaDGATs* and the accumulation of lipids in *B. napus* under low N, drought and salt conditions remain to be further confirmed. Overall, the findings of this study contribute to the understanding of *BnaDGAT* genes in fatty acid biosynthesis and abiotic stress responses in oilseed rape.

Supplementary Materials: The following supporting information can be downloaded at: <https://www.mdpi.com/article/10.3390/plants11091156/s1>, Figure S1: Schematic representation of *DGAT* gene distribution on *Brassica napus*, *Brassica rapa*, and *Brassica oleracea* chromosomes; Figure S2: Gene structures of *DGAT* family members in plants; Figure S3: The conserved motifs of *DGAT* family members in plants; Table S1: Primer sequences for PCR and RT-PCR analysis in this study; Table S2: The corresponding genome databases of *B. napus* and other plant species in this paper; Table S3: The sequences of *DGAT* proteins derived from the corresponding genome databases of *B. napus* and other plant species in this study; Table S4: The CDSs of *DGAT1* genes downloaded from the corresponding genome databases of *B. napus* and other plant species in this study; Table S5: The genomic DNA sequences of *DGAT1* genes downloaded from the corresponding genome databases of *B. napus* and other plant species in this study; Table S6: The sequences of the CDSs, genomic DNAs, proteins and putative promoters of *BnaDGAT* gene members cloned from *B. napus* ZS11 in this study; Table S7: Identification of *DGAT1* subfamily genes in plants; Table S8: Identity matrix of *DGATs* in *B. napus* and three diploid *Brassica* species based on full-length proteins and CDSs; Table S9: The sequences of the putative promoters of *AtDGAT1*, *AtDGAT2* and *AtDGAT3*; Table S10: The cis-acting

regulatory elements in the putative promoters of *BnaDGATs* and *AtDGATs* were analyzed by PlantCARE; Table S11: Transcription factors regulating *BnaDGATs* were predicted using PlantRegMap; Table S12: miRNAs target *B. napus*, *B. rapa* and *A. thaliana* *DGAT* genes. References [115–133] are cited in the supplementary materials.

Author Contributions: Conceptualization, X.Y., X.G., L.H., C.F., R.R.-C.W. and Z.H.; methodology, X.Y., L.H., C.F. and Z.H.; software, X.Y. and C.F.; validation, X.Y., L.H. and C.F.; formal analysis, X.Y. and C.F.; investigation, X.Y., X.G. and L.H.; resources, J.W., C.F. and Z.H.; data curation, X.Y., and C.F.; writing—original draft preparation, X.Y. and X.G.; writing—review and editing, S.L., Y.C., C.F., J.W. and Z.H.; visualization, X.Y., X.G. and C.F.; supervision, R.R.-C.W., C.F. and Z.H.; project administration, X.Y. and C.F.; funding acquisition, Z.H. All authors have read and agreed to the published version of the manuscript.

Funding: This research was funded by the Key Research and Development Project from the Department of Science and Technology of China (2021YFF1000103-4), the Strategic Priority Research Program of the Chinese Academy of Sciences (Grant No. XDA24030502) and the Natural Science Foundation of China (32072095 and 31271755).

Institutional Review Board Statement: Not applicable.

Informed Consent Statement: Not applicable.

Data Availability Statement: Not applicable.

Acknowledgments: The authors thank Nali ZHU in the Laboratory of Proteomics, Institute of Biophysics, Chinese Academy of Sciences, for kindly helping us with GC–MS.

Conflicts of Interest: The authors declare no conflict of interest.

References

- Li, Y.H.; Beisson, F.; Pollard, M.; Ohlrogge, J. Oil content of *Arabidopsis* seeds: The influence of seed anatomy, light and plant-to-plant variation. *Phytochemistry* **2006**, *67*, 904–915. [[CrossRef](#)] [[PubMed](#)]
- Graham, I.A. Seed storage oil mobilization. *Annu. Rev. Plant Biol.* **2008**, *59*, 115–142. [[CrossRef](#)]
- Xu, Y.; Caldo, K.M.P.; Pal-Nath, D.; Ozga, J.; Lemieux, M.J.; Weselake, R.J.; Chen, G.Q. Properties and biotechnological applications of acyl-CoA:diacylglycerol acyltransferase and phospholipid:diacylglycerol acyltransferase from terrestrial plants and microalgae. *Lipids* **2018**, *53*, 663–688. [[CrossRef](#)]
- Liu, Q.; Siloto, R.M.P.; Lehner, R.; Stone, S.J.; Weselake, R.J. Acyl-CoA:diacylglycerol acyltransferase: Molecular biology, biochemistry and biotechnology. *Prog. Lipid Res.* **2012**, *51*, 350–377. [[CrossRef](#)]
- Kennedy, E.P.; Weiss, S.B. Function of cytidine coenzymes in the biosynthesis of phospholipides. *J. Biol. Chem.* **1956**, *222*, 193–214. [[CrossRef](#)]
- Marchive, C.; Nikovics, K.; To, A.; Lepiniec, L.; Baud, S. Transcriptional regulation of fatty acid production in higher plants: Molecular bases and biotechnological outcomes. *Eur. J. Lipid Sci. Technol.* **2014**, *116*, 1332–1343. [[CrossRef](#)]
- Hobbs, D.H.; Lu, C.F.; Hills, M.J. Cloning of a cDNA encoding diacylglycerol acyltransferase from *Arabidopsis thaliana* and its functional expression. *FEBS Lett.* **1999**, *452*, 145–149. [[CrossRef](#)]
- Kroon, J.T.M.; Wei, W.; Simon, W.J.; Slabas, A.R. Identification and functional expression of a type 2 acyl-CoA:diacylglycerol acyltransferase (DGAT2) in developing castor bean seeds which has high homology to the major triglyceride biosynthetic enzyme of fungi and animals. *Phytochemistry* **2006**, *67*, 2541–2549. [[CrossRef](#)] [[PubMed](#)]
- Shockey, J.M.; Gidda, S.K.; Chapital, D.C.; Kuan, J.-C.; Dhanoa, P.K.; Bland, J.M.; Rothstein, S.J.; Mullen, R.T.; Dyer, J.M. Tung tree DGAT1 and DGAT2 have nonredundant functions in triacylglycerol biosynthesis and are localized to different subdomains of the endoplasmic reticulum. *Plant Cell* **2006**, *18*, 2294–2313. [[CrossRef](#)]
- Saha, S.; Enugutti, B.; Rajakumari, S.; Rajasekharan, R. Cytosolic triacylglycerol biosynthetic pathway in oilseeds. Molecular cloning and expression of peanut cytosolic diacylglycerol acyltransferase. *Plant Physiol.* **2006**, *141*, 1533–1543. [[CrossRef](#)]
- Banilas, G.; Karampelias, M.; Makariti, I.; Kourti, A.; Hatzopoulos, P. The olive DGAT2 gene is developmentally regulated and shares overlapping but distinct expression patterns with DGAT1. *J. Exp. Bot.* **2011**, *62*, 521–532. [[CrossRef](#)] [[PubMed](#)]
- Giannoulia, K.; Haralampidis, K.; Poghosyan, Z.; Murphy, D.J.; Hatzopoulos, P. Differential expression of *diacylglycerol acyltransferase* (*DGAT*) genes in olive tissues. *Biochem. Soc. Trans.* **2000**, *28*, 695–697. [[CrossRef](#)] [[PubMed](#)]
- Bouvier-Nave, P.; Benveniste, P.; Oelkers, P.; Sturley, S.L.; Schaller, H. Expression in yeast and tobacco of plant cDNAs encoding acyl CoA:diacylglycerol acyltransferase. *Eur. J. Biochem.* **2000**, *267*, 85–96. [[CrossRef](#)] [[PubMed](#)]
- Chen, B.B.; Wang, J.J.; Zhang, G.Y.; Liu, J.Q.; Manan, S.; Hu, H.H.; Zhao, J. Two types of soybean diacylglycerol acyltransferases are differentially involved in triacylglycerol biosynthesis and response to environmental stresses and hormones. *Sci. Rep.* **2016**, *6*, 28541. [[CrossRef](#)] [[PubMed](#)]

15. Li, R.Z.; Hatanaka, T.; Yu, K.S.; Wu, Y.M.; Fukushige, H.; Hildebrand, D. Soybean oil biosynthesis: Role of diacylglycerol acyltransferases. *Funct. Integr. Genom.* **2013**, *13*, 99–113. [[CrossRef](#)] [[PubMed](#)]
16. Wang, H.W.; Zhang, J.S.; Gai, J.Y.; Chen, S.Y. Cloning and comparative analysis of the gene encoding diacylglycerol acyltransferase from wild type and cultivated soybean. *Theor. Appl. Genet.* **2006**, *112*, 1086–1097. [[CrossRef](#)]
17. Chi, X.Y.; Hu, R.B.; Zhang, X.W.; Chen, M.N.; Chen, N.; Pan, L.J.; Wang, T.; Wang, M.A.; Yang, Z.; Wang, Q.F.; et al. Cloning and functional analysis of three diacylglycerol acyltransferase genes from peanut (*Arachis hypogaea* L.). *PLoS ONE* **2014**, *9*, e105834. [[CrossRef](#)]
18. Peng, Z.Y.; Li, L.; Yang, L.Q.; Zhang, B.; Chen, G.; Bi, Y.P. Overexpression of peanut diacylglycerol acyltransferase 2 in *Escherichia coli*. *PLoS ONE* **2013**, *8*, e61363. [[CrossRef](#)]
19. Nykiforuk, C.L.; Furukawa-Stoffer, T.L.; Huff, P.W.; Sarna, M.; Laroche, A.; Moloney, M.M.; Weselake, R.J. Characterization of cDNAs encoding diacylglycerol acyltransferase from cultures of *Brassica napus* and sucrose-mediated induction of enzyme biosynthesis. *Biochim. Biophys. Acta Mol. Cell Biol. Lipids* **2002**, *1580*, 95–109. [[CrossRef](#)]
20. Aznar-Moreno, J.; Denolf, P.; Van Audenhove, K.; De Bodt, S.; Engelen, S.; Fahy, D.; Wallis, J.G.; Browse, J. Type 1 diacylglycerol acyltransferases of *Brassica napus* preferentially incorporate oleic acid into triacylglycerol. *J. Exp. Bot.* **2015**, *66*, 6497–6506. [[CrossRef](#)]
21. Greer, M.S.; Truksa, M.; Deng, W.; Lung, S.C.; Chen, G.Q.; Weselake, R.J. Engineering increased triacylglycerol accumulation in *Saccharomyces cerevisiae* using a modified type 1 plant diacylglycerol acyltransferase. *Appl. Microbiol. Biotechnol.* **2015**, *99*, 2243–2253. [[CrossRef](#)] [[PubMed](#)]
22. Sun, L.; Ouyang, C.; Kou, S.L.; Wang, S.H.; Yao, Y.Y.; Peng, T.; Xu, Y.; Tang, L.; Chen, F. Cloning and characterization of a cDNA encoding type 1 diacylglycerol acyltransferase from sunflower (*Helianthus annuus* L.). *Z. Naturforsch. C J. Biosci.* **2011**, *66*, 63–72. [[CrossRef](#)] [[PubMed](#)]
23. Xu, J.Y.; Francis, T.; Mietkiewska, E.; Giblin, E.M.; Barton, D.L.; Zhang, Y.; Zhang, M.; Taylor, D.C. Cloning and characterization of an acyl-CoA-dependent diacylglycerol acyltransferase 1 (*DGAT1*) gene from *Tropaeolum majus*, and a study of the functional motifs of the DGAT protein using site-directed mutagenesis to modify enzyme activity and oil content. *Plant Biotechnol. J.* **2008**, *6*, 799–818. [[CrossRef](#)]
24. Zheng, P.; Allen, W.B.; Roesler, K.; Williams, M.E.; Zhang, S.; Li, J.; Glassman, K.; Ranch, J.; Nubel, D.; Solawetz, W.; et al. A phenylalanine in DGAT is a key determinant of oil content and composition in maize. *Nat. Genet.* **2008**, *40*, 367–372. [[CrossRef](#)]
25. Zhao, Y.P.; Wu, N.; Li, W.J.; Shen, J.L.; Chen, C.; Li, F.G.; Hou, Y.X. Evolution and characterization of acetyl coenzyme A: Diacylglycerol acyltransferase genes in cotton identify the roles of *GhDGAT3D* in oil biosynthesis and fatty acid composition. *Genes* **2021**, *12*, 1045. [[CrossRef](#)]
26. Zhang, F.Y.; Yang, M.F.; Xu, Y.N. Silencing of *DGAT1* in tobacco causes a reduction in seed oil content. *Plant Sci.* **2005**, *169*, 689–694. [[CrossRef](#)]
27. Jako, C.; Kumar, A.; Wei, Y.; Zou, J.; Barton, D.L.; Giblin, E.M.; Covello, P.S.; Taylor, D.C. Seed-specific over-expression of an *Arabidopsis* cDNA encoding a diacylglycerol acyltransferase enhances seed oil content and seed weight. *Plant Physiol.* **2001**, *126*, 861–874. [[CrossRef](#)] [[PubMed](#)]
28. Taylor, D.C.; Zhang, Y.; Kumar, A.; Francis, T.; Giblin, E.M.; Barton, D.L.; Ferrie, J.R.; Laroche, A.; Shah, S.; Zhu, W.; et al. Molecular modification of triacylglycerol accumulation by over-expression of *DGAT1* to produce canola with increased seed oil content under field conditions. *Botany* **2009**, *87*, 533–543. [[CrossRef](#)]
29. Maravi, D.K.; Kumar, S.; Sharma, P.K.; Kobayashi, Y.; Goud, V.V.; Sakurai, N.; Koyama, H.; Sahoo, L. Ectopic expression of *AtDGAT1*, encoding diacylglycerol O-acyltransferase exclusively committed to tag biosynthesis, enhances oil accumulation in seeds and leaves of jatropha. *Biotechnol. Biofuels* **2016**, *9*, 226. [[CrossRef](#)] [[PubMed](#)]
30. Lock, Y.Y.; Snyder, C.L.; Zhu, W.M.; Siloto, R.M.P.; Weselake, R.J.; Shah, S. Antisense suppression of type 1 diacylglycerol acyltransferase adversely affects plant development in *Brassica napus*. *Physiol. Plant.* **2009**, *137*, 61–71. [[CrossRef](#)] [[PubMed](#)]
31. Routaboul, J.M.; Benning, C.; Bechtold, N.; Caboche, M.; Lepiniec, L. The *TAG1* locus of *Arabidopsis* encodes for a diacylglycerol acyltransferase. *Plant Physiol. Biochem.* **1999**, *37*, 831–840. [[CrossRef](#)]
32. Kaup, M.T.; Froese, C.D.; Thompson, J.E. A role for diacylglycerol acyltransferase during leaf senescence. *Plant Physiol.* **2002**, *129*, 1616–1626. [[CrossRef](#)] [[PubMed](#)]
33. Zhang, M.; Fan, J.; Taylor, D.C.; Ohlrogge, J.B. *DGAT1* and *PDAT1* acyltransferases have overlapping functions in *Arabidopsis* triacylglycerol biosynthesis and are essential for normal pollen and seed development. *Plant Cell* **2009**, *21*, 3885–3901. [[CrossRef](#)] [[PubMed](#)]
34. Lu, C.; Hills, M.J. *Arabidopsis* mutants deficient in diacylglycerol acyltransferase display increased sensitivity to abscisic acid, sugars, and osmotic stress during germination and seedling development. *Plant Physiol.* **2002**, *129*, 1352–1358. [[CrossRef](#)] [[PubMed](#)]
35. Weselake, R.J.; Shah, S.; Tang, M.; Quant, P.A.; Snyder, C.L.; Furukawastoffer, T.L.; Zhu, W.; Taylor, D.C.; Zou, J.; Kumar, A. Metabolic control analysis is helpful for informed genetic manipulation of oilseed rape (*Brassica napus*) to increase seed oil content. *J. Exp. Bot.* **2008**, *59*, 3543–3549. [[CrossRef](#)] [[PubMed](#)]
36. Yang, Y.; Yu, X.C.; Song, L.F.; An, C.C. ABI4 activates *DGAT1* expression in *Arabidopsis* seedlings during nitrogen deficiency. *Plant Physiol.* **2011**, *156*, 873–883. [[CrossRef](#)]

37. Kelly, A.A.; van Erp, H.; Quettier, A.L.; Shaw, E.; Menard, G.; Kurup, S.; Eastmond, P.J. The SUGAR-DEPENDENT1 lipase limits triacylglycerol accumulation in vegetative tissues of arabidopsis. *Plant Physiol.* **2013**, *162*, 1282–1289. [[CrossRef](#)]
38. Kong, Y.; Chen, S.; Yang, Y.; An, C. ABA-insensitive (ABI) 4 and ABI5 synergistically regulate *DGAT1* expression in *Arabidopsis* seedlings under Stress. *FEBS Lett.* **2013**, *587*, 3076–3082. [[CrossRef](#)]
39. Tjellstrom, H.; Strawsine, M.; Ohlrogge, J.B. Tracking synthesis and turnover of triacylglycerol in leaves. *J. Exp. Bot.* **2015**, *66*, 1453–1461. [[CrossRef](#)]
40. Fan, J.L.; Yu, L.H.; Xu, C.C. A central role for triacylglycerol in membrane lipid breakdown, fatty acid beta-oxidation, and plant survival under extended darkness. *Plant Physiol.* **2017**, *174*, 1517–1530. [[CrossRef](#)] [[PubMed](#)]
41. Arisz, S.A.; Heo, J.Y.; Koevoets, I.T.; Zhao, T.; van Egmond, P.; Meyer, A.J.; Zeng, W.Q.; Niu, X.M.; Wang, B.S.; Mitchell-Olds, T.; et al. Diacylglycerol acyltransferase1 contributes to freezing tolerance. *Plant Physiol.* **2018**, *177*, 1410–1424. [[CrossRef](#)] [[PubMed](#)]
42. Tan, W.J.; Yang, Y.C.; Zhou, Y.; Huang, L.P.; Xu, L.; Chen, Q.F.; Yu, L.J.; Xiao, S. Diacylglycerol acyltransferase and diacylglycerol kinase modulate triacylglycerol and phosphatidic acid production in the plant response to freezing stress. *Plant Physiol.* **2018**, *177*, 1303–1318. [[CrossRef](#)] [[PubMed](#)]
43. Burgal, J.; Shockey, J.; Lu, C.F.; Dyer, J.; Larson, T.; Graham, I.; Browse, J. Metabolic engineering of hydroxy fatty acid production in plants: RcDGAT2 drives dramatic increases in ricinoleate levels in seed oil. *Plant Biotechnol. J.* **2008**, *6*, 819–831. [[CrossRef](#)] [[PubMed](#)]
44. Li, R.Z.; Yu, K.S.; Hatanaka, T.; Hildebrand, D.F. Vernonia DGATs increase accumulation of epoxy fatty acids in oil. *Plant Biotechnol. J.* **2010**, *8*, 184–195. [[CrossRef](#)] [[PubMed](#)]
45. Demski, K.; Jeppson, S.; Lager, I.; Misztak, A.; Jasieniecka-Gazarkiewicz, K.; Waleron, M.; Stymne, S.; Banas, A. Isoforms of acyl-CoA:diacylglycerol acyltransferase2 differ Substantially in their specificities towards erucic acid. *Plant Physiol.* **2019**, *181*, 1468–1479. [[CrossRef](#)] [[PubMed](#)]
46. Ayme, L.; Arragain, S.; Canonge, M.; Baud, S.; Touati, N.; Bimai, O.; Jagic, F.; Louis-Mondesir, C.; Briozzo, P.; Fontecave, M.; et al. *Arabidopsis thaliana* DGAT3 is a [2Fe-2S] protein involved in TAG biosynthesis. *Sci. Rep.* **2018**, *8*, 17254. [[CrossRef](#)] [[PubMed](#)]
47. Hernandez, M.L.; Whitehead, L.; He, Z.S.; Gazda, V.; Gilday, A.; Kozhevnikova, E.; Vaistij, F.E.; Larson, T.R.; Graham, I.A. A cytosolic acyltransferase contributes to triacylglycerol synthesis in sucrose-rescued *Arabidopsis* seed oil catabolism mutants. *Plant Physiol.* **2012**, *160*, 215–225. [[CrossRef](#)] [[PubMed](#)]
48. He, X.H.; Turner, C.; Chen, G.Q.; Lin, J.T.; McKeon, T.A. Cloning and characterization of a cDNA encoding diacylglycerol acyltransferase from castor bean. *Lipids* **2004**, *39*, 311–318. [[CrossRef](#)]
49. Lu, C.F.L.; de Noyer, S.B.; Hobbs, D.H.; Kang, J.L.; Wen, Y.C.; Krachtus, D.; Hills, M.J. Expression pattern of diacylglycerol acyltransferase-1, an enzyme involved in triacylglycerol biosynthesis, in *Arabidopsis thaliana*. *Plant Mol. Biol.* **2003**, *52*, 31–41. [[CrossRef](#)]
50. Zhao, C.Z.; Li, H.; Zhang, W.X.; Wang, H.L.; Xu, A.X.; Tian, J.H.; Zou, J.T.; Taylor, D.C.; Zhang, M. BnDGAT1s function similarly in oil deposition and are expressed with uniform patterns in tissues of *Brassica napus*. *Front. Plant Sci.* **2017**, *8*, 2205. [[CrossRef](#)] [[PubMed](#)]
51. Uagaharu, N. Genomic analysis of *Brassica* with special reference to the experimental formation of *B. napus* and peculiar mode of fertilization. *Jpn. J. Bot.* **1935**, *7*, 389–452.
52. Snowdon, R.J. Cytogenetics and genome analysis in *Brassica* crops. *Chromosome Res.* **2007**, *15*, 85–95. [[CrossRef](#)] [[PubMed](#)]
53. Chalhoub, B.; Denoeud, F.; Liu, S.Y.; Parkin, I.A.P.; Tang, H.B.; Wang, X.Y.; Chiquet, J.; Belcram, H.; Tong, C.B.; Samans, B.; et al. Early allopolyploid evolution in the post-neolithic *Brassica napus* oilseed genome. *Science* **2014**, *345*, 950–953. [[CrossRef](#)]
54. Ostergaard, L.; King, G.J. Standardized gene nomenclature for the *Brassica* genus. *Plant Methods* **2008**, *4*, 10. [[CrossRef](#)]
55. Cheng, F.; Wu, J.; Wang, X.W. Genome triplication drove the diversification of *Brassica* plants. *Hortic. Res.* **2014**, *1*, 14024. [[CrossRef](#)]
56. Hu, B.; Jin, J.P.; Guo, A.Y.; Zhang, H.; Luo, J.C.; Gao, G. GSDS 2.0: An upgraded gene feature visualization server. *Bioinformatics* **2015**, *31*, 1296–1297. [[CrossRef](#)]
57. Lu, S.N.; Wang, J.Y.; Chitsaz, F.; Derbyshire, M.K.; Geer, R.C.; Gonzales, N.R.; Gwadz, M.; Hurwitz, D.I.; Marchler, G.H.; Song, J.S.; et al. CDD/SPARCLE: The conserved domain database in 2020. *Nucleic Acids Res.* **2020**, *48*, D265–D268. [[CrossRef](#)]
58. Krogh, A.; Larsson, B.; von Heijne, G.; Sonnhammer, E.L.L. Predicting transmembrane protein topology with a hidden markov model: Application to complete genomes. *J. Mol. Biol.* **2001**, *305*, 567–580. [[CrossRef](#)]
59. Sandager, L.; Gustavsson, M.H.; Stahl, U.; Dahlqvist, A.; Wiberg, E.; Banas, A.; Lenman, M.; Ronne, H.; Stymne, S. Storage lipid synthesis is non-essential in yeast. *J. Biol. Chem.* **2002**, *277*, 6478–6482. [[CrossRef](#)] [[PubMed](#)]
60. Liu, D.; Yu, L.; Wei, L.; Yu, P.; Wang, J.; Zhao, H.; Zhang, Y.; Zhang, S.; Yang, Z.; Chen, G.; et al. BnTIR: An online transcriptome platform for exploring RNA-seq libraries for oil crop *Brassica napus*. *Plant Biotechnol. J.* **2021**, *19*, 1895–1897. [[CrossRef](#)]
61. Chao, H.; Li, T.; Luo, C.; Huang, H.; Ruan, Y.; Li, X.; Niu, Y.; Fan, Y.; Sun, W.; Zhang, K.; et al. BrassicaEDB: A gene expression database for *Brassica* crops. *Int. J. Mol. Sci.* **2020**, *21*, 5831. [[CrossRef](#)] [[PubMed](#)]
62. Chen, C.; Chen, H.; Zhang, Y.; Thomas, H.R.; Frank, M.H.; He, Y.; Xia, R. TBtools: An integrative toolkit developed for interactive analyses of big biological data. *Mol. Plant* **2020**, *13*, 1194–1202. [[CrossRef](#)] [[PubMed](#)]
63. Noman, A.; Fahad, S.; Aqeel, M.; Ali, U.; Amanullah; Anwar, S.; Baloch, S.K.; Zainab, M. miRNAs: Major modulators for crop growth and development under abiotic stresses. *Biotechnol. Lett.* **2017**, *39*, 685–700. [[CrossRef](#)]

64. Khraiweh, B.; Zhu, J.K.; Zhu, J.H. Role of miRNAs and siRNAs in biotic and abiotic stress responses of plants. *Biochim. Biophys. Acta Gene Regul. Mech.* **2012**, *1819*, 137–148. [[CrossRef](#)]
65. Turchetto-Zolet, A.C.; Christoff, A.P.; Kulcheski, F.R.; Loss-Morais, G.; Margis, R.; Margis-Pinheiro, M. Diversity and evolution of plant diacylglycerol acyltransferase (DGATs) unveiled by phylogenetic, gene structure and expression analyses. *Genet. Mol. Biol.* **2016**, *39*, 524–538. [[CrossRef](#)] [[PubMed](#)]
66. Weselake, R.J.; Madhavji, M.; Szarka, S.J.; Patterson, N.A.; Wiehler, W.B.; Nykiforuk, C.L.; Burton, T.L.; Boora, P.S.; Mosimann, S.C.; Foroud, N.A.; et al. Acyl-CoA-binding and self-associating properties of a recombinant 13.3 kDa N-terminal fragment of diacylglycerol acyltransferase-1 from oilseed rape. *BMC Biochem.* **2006**, *7*, 24. [[CrossRef](#)] [[PubMed](#)]
67. Caldo, K.M.P.; Greer, M.S.; Chen, G.Q.; Lemieux, M.J.; Weselake, R.J. Purification and properties of recombinant *Brassica napus* diacylglycerol acyltransferase 1. *FEBS Lett.* **2015**, *589*, 773–778. [[CrossRef](#)] [[PubMed](#)]
68. Liu, D.; Ji, H.; Yang, Z. Functional characterization of three novel genes encoding diacylglycerol acyltransferase (DGAT) from oil-rich tubers of *Cyperus esculentus*. *Plant Cell Physiol.* **2020**, *61*, 118–129. [[CrossRef](#)] [[PubMed](#)]
69. Zhou, X.R.; Shrestha, P.; Yin, F.; Petrie, J.R.; Singh, S.P. AtDGAT2 is a functional acyl-CoA:diacylglycerol acyltransferase and displays different acyl-CoA substrate preferences than AtDGAT1. *FEBS Lett.* **2013**, *587*, 2371–2376. [[CrossRef](#)] [[PubMed](#)]
70. Chen, Y.; Cui, Q.; Xu, Y.; Yang, S.; Gao, M.; Wang, Y. Effects of tung oilseed *FAD2* and *DGAT2* genes on unsaturated fatty acid accumulation in *Rhodotorula glutinis* and *Arabidopsis thaliana*. *Mol. Genet. Genom.* **2015**, 1605–1613. [[CrossRef](#)] [[PubMed](#)]
71. Kainou, K.; Kamisaka, Y.; Kimura, K.; Uemura, H. Isolation of $\Delta 12$ and $\omega 3$ -fatty acid desaturase genes from the yeast *Kluyveromyces lactis* and their heterologous expression to produce linoleic and α -linolenic acids in *Saccharomyces cerevisiae*. *Yeast* **2006**, *23*, 605–612. [[CrossRef](#)] [[PubMed](#)]
72. Gao, H.; Gao, Y.; Zhang, F.; Liu, B.; Ji, C.; Xue, J.; Yuan, L.; Li, R. Functional characterization of a novel acyl-CoA:diacylglycerol acyltransferase 3-3 (CsDGAT3-3) gene from *Camelina sativa*. *Plant Sci.* **2021**, *303*, 110752. [[CrossRef](#)]
73. Yan, B.W.; Xu, X.X.; Gu, Y.N.; Zhao, Y.; Zhao, X.C.; He, L.; Zhao, C.J.; Li, Z.T.; Xu, J.Y. Genome-wide characterization and expression profiling of diacylglycerol acyltransferase genes from maize. *Genome* **2018**, *61*, 735–743. [[CrossRef](#)] [[PubMed](#)]
74. Zhao, Y.P.; Wang, Y.M.; Huang, Y.; Cui, Y.P.; Hua, J.P. Gene network of oil accumulation reveals expression profiles in developing embryos and fatty acid composition in upland cotton. *J. Plant Physiol.* **2018**, *228*, 101–112. [[CrossRef](#)] [[PubMed](#)]
75. Sajjadi, B.; Chen, W.Y.; Raman, A.A.A.; Ibrahim, S. Microalgae lipid and biomass for biofuel production: A comprehensive review on lipid enhancement strategies and their effects on fatty acid composition. *Renew. Sustain. Energy Rev.* **2018**, *97*, 200–232. [[CrossRef](#)]
76. Liang, K.H.; Zhang, Q.H.; Gu, M.; Cong, W. Effect of phosphorus on lipid accumulation in freshwater microalga *Chlorella* sp. *J. Appl. Phycol.* **2013**, *25*, 311–318. [[CrossRef](#)]
77. Li, X.; Hu, H.Y.; Gan, K.; Sun, Y.X. Effects of different nitrogen and phosphorus concentrations on the growth, nutrient uptake, and lipid accumulation of a freshwater microalga *Scenedesmus* sp. *Bioresour. Technol.* **2010**, *101*, 5494–5500. [[CrossRef](#)]
78. Khozin-Goldberg, I.; Cohen, Z. The effect of phosphate starvation on the lipid and fatty acid composition of the fresh water eustigmatophyte *Monodus subterraneus*. *Phytochemistry* **2006**, *67*, 696–701. [[CrossRef](#)]
79. Guschina, I.A.; Dobson, G.; Harwood, J.L. Lipid metabolism in cultured lichen photobionts with different phosphorus status. *Phytochemistry* **2003**, *64*, 209–217. [[CrossRef](#)]
80. Markou, G.; Chatzipavlidis, I.; Georgakakis, D. Carbohydrates production and bio-flocculation characteristics in cultures of *Arthrospira (Spirulina) platensis*: Improvements through phosphorus limitation process. *Bioenergy Res.* **2012**, *5*, 915–925. [[CrossRef](#)]
81. Shimojima, M.; Madoka, Y.; Fujiwara, R.; Murakawa, M.; Yoshitake, Y.; Ikeda, K.; Koizumi, R.; Endo, K.; Ozaki, K.; Ohta, H. An engineered lipid remodeling system using a galactolipid synthase promoter during phosphate starvation enhances oil accumulation in plants. *Front. Plant Sci.* **2015**, *6*, 664. [[CrossRef](#)] [[PubMed](#)]
82. Pant, B.D.; Burgos, A.; Pant, P.; Cuadros-Inostroza, A.; Willmitzer, L.; Scheible, W.R. The transcription factor PHR1 regulates lipid remodeling and triacylglycerol accumulation in *Arabidopsis thaliana* during phosphorus starvation. *J. Exp. Bot.* **2015**, *66*, 1907–1918. [[CrossRef](#)] [[PubMed](#)]
83. Chen, G.Q.; Xu, Y.; Siloto, R.M.P.; Caldo, K.M.P.; Vanhercke, T.; El Tahchy, A.; Niesner, N.; Chen, Y.Y.; Mietkiewska, E.; Weselake, R.J. High-performance variants of plant diacylglycerol acyltransferase 1 generated by directed evolution provide insights into structure function. *Plant J.* **2017**, *92*, 167–177. [[CrossRef](#)]
84. Caldo, K.M.P.; Shen, W.; Xu, Y.; Hanley-Bowdoin, L.; Chen, G.Q.; Weselake, R.J.; Lemieux, M.J. Diacylglycerol acyltransferase 1 is activated by phosphatidate and inhibited by SnRK1-catalyzed phosphorylation. *Plant J.* **2018**, *96*, 287–299. [[CrossRef](#)] [[PubMed](#)]
85. Cruz-Ramirez, A.; Oropeza-Aburto, A.; Razo-Hernandez, F.; Ramirez-Chavez, E.; Herrera-Estrella, L. Phospholipase DZ2 plays an important role in extraplastidic galactolipid biosynthesis and phosphate recycling in *Arabidopsis* roots. *Proc. Natl. Acad. Sci. USA* **2006**, *103*, 6765–6770. [[CrossRef](#)] [[PubMed](#)]
86. Oropeza-Aburto, A.; Cruz-Ramirez, A.; Acevedo-Hernandez, G.J.; Perez-Torres, C.A.; Caballero-Perez, J.; Herrera-Estrella, L. Functional analysis of the *Arabidopsis* PLDZ2 promoter reveals an evolutionarily conserved low-pi-responsive transcriptional enhancer element. *J. Exp. Bot.* **2012**, *63*, 2189–2202. [[CrossRef](#)] [[PubMed](#)]
87. Fragoso, S.; Espindola, L.; Paez-Valencia, J.; Gamboa, A.; Camacho, Y.; Martinez-Barajas, E.; Coello, P. SnRK1 Isoforms AKIN10 and AKIN11 are differentially regulated in *Arabidopsis* plants under phosphate starvation. *Plant Physiol.* **2009**, *149*, 1906–1916. [[CrossRef](#)]

88. Deng, X.D.; Li, Y.J.; Fei, X.W. The mRNA abundance of *pepc2* gene is negatively correlated with oil content in *Chlamydomonas reinhardtii*. *Biomass Bioenergy* **2011**, *35*, 1811–1817. [[CrossRef](#)]
89. Illman, A.M.; Scragg, A.H.; Shales, S.W. Increase in *Chlorella* strains calorific values when grown in low nitrogen medium. *Enzym. Microb. Technol.* **2000**, *27*, 631–635. [[CrossRef](#)]
90. Rodolfi, L.; Zittelli, G.C.; Bassi, N.; Padovani, G.; Biondi, N.; Bonini, G.; Tredici, M.R. Microalgae for oil: Strain selection, induction of lipid synthesis and outdoor mass cultivation in a low-cost photobioreactor. *Biotechnol. Bioeng.* **2009**, *102*, 100–112. [[CrossRef](#)]
91. Spoehr, H.A.; Milner, H.W. The chemical composition of chlorella; effect of environmental conditions. *Plant Physiol.* **1949**, *24*, 120–149. [[CrossRef](#)]
92. Guo, X.J.; Fan, C.M.; Chen, Y.H.; Wang, J.Q.; Yin, W.B.; Wang, R.R.C.; Hu, Z.M. Identification and characterization of an efficient acyl-CoA: Diacylglycerol acyltransferase 1 (*DGAT1*) gene from the microalga *Chlorella ellipsoidea*. *BMC Plant Biol.* **2017**, *17*, 48. [[CrossRef](#)] [[PubMed](#)]
93. Adams, C.; Godfrey, V.; Wahlen, B.; Seefeldt, L.; Bugbee, B. Understanding precision nitrogen stress to optimize the growth and lipid cross mark content tradeoff in oleaginous green microalgae. *Bioresour. Technol.* **2013**, *131*, 188–194. [[CrossRef](#)] [[PubMed](#)]
94. Kumar, R.; Biswas, K.; Singh, P.K.; Singh, P.K.; Elumalai, S.; Shukla, P.; Pabbi, S. Lipid production and molecular dynamics simulation for regulation of *accD* gene in cyanobacteria under different N and P regimes. *Biotechnol. Biofuels* **2017**, *10*, 94. [[CrossRef](#)] [[PubMed](#)]
95. Martin, T.; Oswald, O.; Graham, I.A. *Arabidopsis* seedling growth, storage lipid mobilization, and photosynthetic gene expression are regulated by carbon; nitrogen availability. *Plant Physiol.* **2002**, *128*, 472–481. [[CrossRef](#)] [[PubMed](#)]
96. Gaude, N.; Brehelin, C.; Tischendorf, G.; Kessler, F.; Dormann, P. Nitrogen deficiency in *Arabidopsis* affects galactolipid composition and gene expression and results in accumulation of fatty acid phytyl esters. *Plant J.* **2007**, *49*, 729–739. [[CrossRef](#)]
97. Eastmond, P.J.; Germain, V.; Lange, P.R.; Bryce, J.H.; Smith, S.M.; Graham, I.A. Postgerminative growth and lipid catabolism in oilseeds lacking the glyoxylate cycle. *Proc. Natl. Acad. Sci. USA* **2000**, *97*, 5669–5674. [[CrossRef](#)] [[PubMed](#)]
98. Svenningsson, H.; Liljenberg, C. Membrane lipid changes in root cells of rape (*Brassica napus*) as a function of water-deficit stress. *Physiol. Plant.* **1986**, *68*, 53–58. [[CrossRef](#)]
99. Dakhma, W.S.; Zarrouk, M.; Cherif, A. Effects of drought-stress on lipids in rape leaves. *Phytochemistry* **1995**, *40*, 1383–1386. [[CrossRef](#)]
100. Aziz, A.; Larher, F. Osmotic stress induced changes in lipid composition and peroxidation in leaf discs of *Brassica napus* L. *J. Plant Physiol.* **1998**, *153*, 754–762. [[CrossRef](#)]
101. Aslam, M.N.; Nelson, M.N.; Kailis, S.G.; Bayliss, K.L.; Speijers, J.; Cowling, W.A. Canola oil increases in polyunsaturated fatty acids and decreases in oleic acid in drought-stressed Mediterranean-type environments. *Plant Breed.* **2009**, *128*, 348–355. [[CrossRef](#)]
102. Douglas, T.J.; Paleg, L.G. Lipid composition of *Zea mays* seedlings and water stress-induced changes. *J. Exp. Bot.* **1981**, *32*, 499–508. [[CrossRef](#)]
103. Martin, B.A.; Schoper, J.B.; Rinne, R.W. Changes in soybean (*Glycine max* [L.] Merr) glycerolipids in response to water-stress. *Plant Physiol.* **1986**, *81*, 798–801. [[CrossRef](#)]
104. Thi, A.T.P.; Borrellood, C.; Dasilva, J.V.; Justin, A.M.; Mazliak, P. Effects of water stress on lipid metabolism in cotton leaves. *Phytochemistry* **1985**, *24*, 723–727. [[CrossRef](#)]
105. Urao, T.; Yamaguchishinozaki, K.; Urao, S.; Shinozaki, K. An *Arabidopsis* myb homolog is induced by dehydration stress and its gene product binds to the conserved MYB recognition sequence. *Plant Cell* **1993**, *5*, 1529–1539. [[CrossRef](#)]
106. Xu, Z.W.; Wang, M.P.; Guo, Z.T.; Zhu, X.F.; Xia, Z.L. Identification of a 119-bp promoter of the maize sulfite oxidase gene (*ZmSO*) that confers high-level gene expression and ABA or drought inducibility in transgenic plants. *Int. J. Mol. Sci.* **2019**, *20*, 3326. [[CrossRef](#)]
107. Abe, H.; Urao, T.; Ito, T.; Seki, M.; Shinozaki, K.; Yamaguchi-Shinozaki, K. *Arabidopsis* AtMYC2 (bHLH) and AtMYB2 (MYB) function as transcriptional activators in abscisic acid signaling. *Plant Cell* **2003**, *15*, 63–78. [[CrossRef](#)]
108. Wei, L.; Zhu, Y.; Liu, R.; Zhang, A.; Zhu, M.; Xu, W.; Lin, A.; Lu, K.; Li, J. Genome wide identification and comparative analysis of glutathione transferases (GST) family genes in *Brassica napus*. *Sci. Rep.* **2019**, *9*, 9196. [[CrossRef](#)]
109. Bailey, T.L.; Boden, M.; Buske, F.A.; Frith, M.; Grant, C.E.; Clementi, L.; Ren, J.; Li, W.W.; Noble, W.S. MEME SUITE: Tools for motif discovery and searching. *Nucleic Acids Res.* **2009**, *37*, W202–W208. [[CrossRef](#)]
110. Hoagland, D.R.; Arnon, D.I. The water culture method for growing plants without soil. *Calif. Agric. Exp. Stn. Bull.* **1938**, *347*, 36–39.
111. Rogers, S.O.; Bendich, A.J. Extraction of DNA from milligram amounts of fresh, herbarium and mummified plant tissues. *Plant Mol. Biol.* **1985**, *5*, 69–76. [[CrossRef](#)] [[PubMed](#)]
112. Tian, F.; Yang, D.C.; Meng, Y.Q.; Jin, J.; Gao, G. PlantRegMap: Charting functional regulatory maps in plants. *Nucleic Acids Res.* **2020**, *48*, D1104–D1113. [[CrossRef](#)] [[PubMed](#)]
113. Dai, X.; Zhuang, Z.; Zhao, P.X. psRNATarget: A plant small RNA target analysis server (2017 release). *Nucleic Acids Res.* **2018**, *46*, W49–W54. [[CrossRef](#)] [[PubMed](#)]
114. Lescot, M.; Dehais, P.; Thijs, G.; Marchal, K.; Moreau, Y.; Van de Peer, Y.; Rouze, P.; Rombauts, S. PlantCARE, a database of plant *cis*-acting regulatory elements and a portal to tools for in silico analysis of promoter sequences. *Nucleic Acids Res.* **2002**, *30*, 325–327. [[CrossRef](#)] [[PubMed](#)]

115. Zhuang, W.J.; Chen, H.; Yang, M.; Wang, J.P.; Pandey, M.K.; Zhang, C.; Chang, W.C.; Zhang, L.S.; Zhang, X.T.; Tang, R.H.; et al. The genome of cultivated peanut provides insight into legume karyotypes, polyploid evolution and crop domestication. *Nat. Genet.* **2019**, *51*, 865–876. [[CrossRef](#)]
116. Kaul, S.; Koo, H.L.; Jenkins, J.; Rizzo, M.; Rooney, T.; Tallon, L.J.; Feldblyum, T.; Nierman, W.; Benito, M.I.; Lin, X.Y.; et al. Analysis of the genome sequence of the flowering plant *Arabidopsis thaliana*. *Nature* **2000**, *408*, 796–815. [[CrossRef](#)]
117. Huala, E.; Dickerman, A.W.; Garcia-Hernandez, M.; Weems, D.; Reiser, L.; LaFond, F.; Hanley, D.; Kiphart, D.; Zhuang, M.; Huang, W.; et al. The Arabidopsis Information Resource (TAIR): A comprehensive database and web-based information retrieval, analysis, and visualization system for a model plant. *Nucleic Acids Res.* **2001**, *29*, 102–105. [[CrossRef](#)]
118. Vogel, J.P.; Garvin, D.F.; Mockler, T.C.; Schmutz, J.; Rokhsar, D.; Bevan, M.W.; Barry, K.; Lucas, S.; Harmon-Smith, M.; Lail, K.; et al. Genome sequencing and analysis of the model grass *Brachypodium distachyon*. *Nature* **2010**, *463*, 763–768. [[CrossRef](#)]
119. Yang, J.; Liu, D.; Wang, X.; Ji, C.; Cheng, F.; Liu, B.; Hu, Z.; Chen, S.; Pental, D.; Ju, Y.; et al. The genome sequence of allopolyploid *Brassica juncea* and analysis of differential homoeolog gene expression influencing selection. *Nat. Genet.* **2016**, *48*, 1225–1232. [[CrossRef](#)] [[PubMed](#)]
120. Rousseau-Gueutin, M.; Belser, C.; Da Silva, C.; Richard, G.; Istace, B.; Cruaud, C.; Falentin, C.; Boideau, F.; Boutte, J.; Delourme, R.; et al. Long-read assembly of the *Brassica napus* reference genome Darmor-bzh. *GigaScience* **2020**, *9*, 1–16. [[CrossRef](#)] [[PubMed](#)]
121. Perumal, S.; Koh, C.S.; Jin, L.; Buchwaldt, M.; Higgins, E.; Zheng, C.; Sankoff, D.; Robinson, S.J.; Kagale, S.; Navabi, Z.-K.; et al. High contiguity long read assembly of *Brassica nigra* allows localization of active centromeres and provides insights into the ancestral *Brassica* genome. *bioRxiv* **2020**. [[CrossRef](#)]
122. Zhang, L.; Cai, X.; Wu, J.; Liu, M.; Grob, S.; Cheng, F.; Liang, J.; Cai, C.; Liu, Z.; Liu, B.; et al. Improved *Brassica rapa* reference genome by single-molecule sequencing and chromosome conformation capture technologies. *Hortic. Res.* **2018**, *5*, 50. [[CrossRef](#)] [[PubMed](#)]
123. Cai, X.; Wu, J.; Liang, J.; Lin, R.; Zhang, K.; Cheng, F.; Wang, X. Improved *Brassica oleracea* JZS assembly reveals significant changing of LTR-RT dynamics in different morphotypes. *Theor. Appl. Genet.* **2020**, *133*, 3187–3199. [[CrossRef](#)] [[PubMed](#)]
124. Schmutz, J.; Cannon, S.B.; Schlueter, J.; Ma, J.X.; Mitros, T.; Nelson, W.; Hyten, D.L.; Song, Q.J.; Thelen, J.J.; Cheng, J.L.; et al. Genome sequence of the palaeopolyploid soybean. *Nature* **2010**, *463*, 178–183. [[CrossRef](#)] [[PubMed](#)]
125. Valliyodan, B.; Cannon, S.B.; Bayer, P.E.; Shu, S.Q.; Brown, A.V.; Ren, L.H.; Jenkins, J.; Chung, C.Y.L.; Chan, T.F.; Daum, C.G.; et al. Construction and comparison of three reference-quality genome assemblies for soybean. *Plant J.* **2019**, *100*, 1066–1082. [[CrossRef](#)] [[PubMed](#)]
126. Sato, S.; Hirakawa, H.; Isobe, S.; Fukai, E.; Watanabe, A.; Kato, M.; Kawashima, K.; Minami, C.; Muraki, A.; Nakazaki, N.; et al. Sequence analysis of the genome of an oil-bearing tree, *Jatropha curcas* L. *DNA Res.* **2011**, *18*, 65–76. [[CrossRef](#)] [[PubMed](#)]
127. Tang, H.B.; Krishnakumar, V.; Bidwell, S.; Rosen, B.; Chan, A.N.; Zhou, S.G.; Gentzbittel, L.; Childs, K.L.; Yandell, M.; Gundlach, H.; et al. An improved genome release (version Mt4.0) for the model legume *Medicago truncatula*. *BMC Genom.* **2014**, *15*, 312. [[CrossRef](#)] [[PubMed](#)]
128. Ouyang, S.; Zhu, W.; Hamilton, J.; Lin, H.; Campbell, M.; Childs, K.; Thibaud-Nissen, F.; Malek, R.L.; Lee, Y.; Zheng, L.; et al. The TIGR Rice Genome Annotation Resource: Improvements and new features. *Nucleic Acids Res.* **2007**, *35*, D883–D887. [[CrossRef](#)] [[PubMed](#)]
129. Chan, A.P.; Crabtree, J.; Zhao, Q.; Lorenzi, H.; Orvis, J.; Puiiu, D.; Melake-Berhan, A.; Jones, K.M.; Redman, J.; Chen, G.; et al. Draft genome sequence of the oilseed species *Ricinus communis*. *Nat. Biotechnol.* **2010**, *28*, 951–956. [[CrossRef](#)] [[PubMed](#)]
130. Xu, W.; Wu, D.; Yang, T.; Sun, C.; Wang, Z.; Han, B.; Wu, S.; Yu, A.; Chapman, M.A.; Muraguri, S.; et al. Genomic insights into the origin, domestication and genetic basis of agronomic traits of castor bean. *Genome Biol.* **2021**, *22*, 113. [[CrossRef](#)] [[PubMed](#)]
131. Zhang, G.Y.; Liu, X.; Quan, Z.W.; Cheng, S.F.; Xu, X.; Pan, S.K.; Xie, M.; Zeng, P.; Yue, Z.; Wang, W.L.; et al. Genome sequence of foxtail millet (*Setaria italica*) provides insights into grass evolution and biofuel potential. *Nat. Biotechnol.* **2012**, *30*, 549–554. [[CrossRef](#)]
132. Bennetzen, J.L.; Schmutz, J.; Wang, H.; Percifield, R.; Hawkins, J.; Pontaroli, A.C.; Estep, M.; Feng, L.; Vaughn, J.N.; Grimwood, J.; et al. Reference genome sequence of the model plant *Setaria*. *Nat. Biotechnol.* **2012**, *30*, 555–561. [[CrossRef](#)] [[PubMed](#)]
133. Bornowski, N.; Michel, K.J.; Hamilton, J.P.; Ou, S.J.; Seetharam, A.S.; Jenkins, J.; Grimwood, J.; Plott, C.; Shu, S.Q.; Talag, J.; et al. Genomic variation within the maize stiff-stalk heterotic germplasm pool. *Plant Genome* **2021**. [[CrossRef](#)] [[PubMed](#)]